AUTOPHAGY IN TISSUE HOMEOSTASIS AND CANCER

by

GIZEM KARSLI UZUNBAS

A Dissertation submitted to the

Graduate School-New Brunswick

Rutgers, The State University of New Jersey

in partial fulfillment of the requirements

for the degree of

Doctor of Philosophy

Graduate Program in Biochemistry

written under the direction of

Dr. Eileen White

and approved by

_____

_____

_____

_____

_____

New Brunswick, New Jersey

JANUARY, 2015

ABSTRACT OF THE DISSERTATION

Requirement of Autophagy in Health and Cancer

By Gizem Karsli Uzunbas

Dissertation Director:
Dr. Eileen White

Macroautophagy (autophagy hereafter) is a protective process that recycles cellular components to maintain homeostasis and survival. By removing damaged protein and organelles, autophagy ensures protein and organelle quality control. In cancer, the role of autophagy is context dependent. Autophagy is an essential survival mechanism during starvation that promotes tumor progression, but there are also cases where autophagy can suppress tumorigenesis in mouse models. Thus, understanding the role of autophagy modulation in cancer is critical for cancer therapy.

Tumors with RAS mutations require autophagy to tolerate metabolic stress, suggesting that autophagy inhibition may be a potential approach in cancer therapy. However, how systemic autophagy inactivation differentially affects normal and tumor tissues is unknown. To assess the functional significance of autophagy, we conditionally deleted the essential autophagy gene, *Atg7*, throughout adult mice. In that way, we could model the consequences of

autophagy inactivation simultaneously to both normal and tumor tissue to simulate autophagy inhibition in cancer therapy.

First, we wanted to identify what happens to an adult mouse when autophagy is turned off. We generated a mouse model to delete *Atg7*, throughout the entire mouse to determine the role of autophagy in adult mammal. Systemic ATG7 ablation caused susceptibility to infection and neurodegeneration that limited survival to 2-3 months. Moreover, autophagy was required to maintain fat stores and to mobilize free fatty acids specifically in response to fasting. Also, upon fasting, autophagy-deficient mice suffered muscle wasting and fatal hypoglycemia that is mediated by p53. Not only limited to the starvation stress response, inhibiting autophagy also increased sensitivity to γ-irradiation-induced death.

Second, knowing that there is a window of time that adult mice can survive without autophagy, we examined if autophagy ablation is selectively toxic to tumors while sparing normal tissues. For this purpose, we generated another mouse model to induce non-small-cell lung cancer (NSCLC) and then prior to or once tumors were established, we acutely ablated autophagy. Prior autophagy ablation did not alter the efficiency of NSCLC initiation by activation of oncogenic $Kras^{G12D}$ and deletion of the *Trp53* tumor suppressor. Acute autophagy ablation in mice with pre-existing NSCLC, however, blocked tumor growth, promoted tumor cell death, and generated more benign cancer with oncocytic changes. Moreover, host autophagy contributed to tumor growth. This anti-tumor activity

occurred prior to destruction of normal tissues, suggesting that, acute autophagy inhibition may be therapeutically beneficial in cancer.

PREFACE

Parts of this research were originally published in *Cancer Discovery*.

Karsli-Uzunbas, G., Guo, J.Y., Price, S., Teng, X., Laddha, S.V., Khor, S., Kalaany, N.Y., Jacks, T., Chan, C.S., Rabinowitz, J.D.*, et al.* (2014). Autophagy is required for glucose homeostasis and lung tumor maintenance. *Cancer Discovery* 4, 914-927.

ACKNOWLEDGEMENTS

This dissertation would not have existed without support from many people: my mentors, lab-mates, colleagues, friends and family. I would like to thank these people for their contributions to my academic life.

First of all, I would like to thank my advisor, Eileen White, for her guidance, which started even before I joined her lab. All her advice was always valuable to me and will always be. She did not only provide scholarly support, but also personal support whenever she could. Her high expectations, although challenging at times, and her curiosity motivated me throughout my study. I feel lucky for being involved in such a great project and for everything I learned from such a knowledgeable mentor and teacher. Eileen, thank you for everything.

I would like to thank Josh Rabinowitz, for being in my committee and for his enormous guidance with constructive feedbacks. I am also grateful for his positive attitude at all times. I would also like to acknowledge my other committee members: Vassiliki Karantza, Bing Xia and Shengkan (Victor) Jin for their time, valuable feedbacks and suggestions. I also would like to mention Nada Kalaany for her constructive and helpful ideas.

I feel extremely lucky to work with wonderful lab-mates. First, I would like to mention Jessie. I started to work with her as a rotation student when I first joined the White Lab. Other than basic lab skills, she taught me that nothing is difficult and there is always alternative ways. She was my second mentor, right hand, cheering sister and guiding mother whenever I needed. I am also grateful to Sandy, my left hand, mouse whisperer, laughter-mate. I thank both of them not

only improving my work, but also improving my life. They will be in my life wherever I am. My special thanks go to Shilpy and Anne, for their moral and technical support. Thanks also to former lab members Kevin and Sinan, for their support. I would like to thank Yang, Xiaoqi, Urmila and Keeah. Without their endless help, this thesis will be incomplete.

I also need to thank all CINJ staff for helpful collaborations; in particular, Saurabh and Chang Chan for gene expression analysis, Xin from Princeton University for metabolomic analysis, Neil for *in vivo* imaging, Yanying for radiation experiments, TAS and the vivarium staff for their helps.

I owe many thanks to my wonderful friends, who made thousands miles away my home. The tough moments of these five years made me realize one more time what a big family we are. I am grateful to Bahar, Birnur, Erhan, Erman, Gokce, Gulsad, Kubra, Sarp, Selen, Turgay, Zafer and Zuhal. Thanks for all the support and distractions; we shared laughter and tears; and we have many more to be shared, they will always be in my life.

Lastly, my most heartfelt gratitude goes to my family; my beloved, supporting and cheering parents, Melek and Mustafa; my precious, best friend, brother, Barkin; my motivating and advisor sister, Elif; joy and love of my life, my little nephew, Eren; beloved and encouring parents, Fatma and Abdullah; my overseas intimate friend for 20 years, my precious, Gunce. My special thanks go to my beloved husband, love, best friend, Gokhan, for being on my side all these years. I thank him for making me laugh and laughing with me, listening constantly and supporting unconditionally.

DEDICATION

This dissertation is dedicated to people for whose existence I am grateful for, always:

My beloved mom, Melek; my dad, Mustafa and my brother, Barkin,

And my love Gokhan,

And those who attempt to change the world.

TABLE OF CONTENTS

LIST OF FIGURES

LIST OF ABBREVIATIONS

Ad-FlpO:	adenovirus expressing Flp recombinase
AMBRA1:	activating molecule in Beclin1-regulated autophagy
AMPK:	AMP activated protein kinase
AREs	antioxidant response elements
ATG:	autophagy-related
BAT:	brown adipose tissue
BCL-2:	B-cell lymphoma 2
BCL-XL:	B-cell lymphoma extra large
BECN1:	BECLIN-1; BCL-2 interacting protein
BIF-1:	Bax-interacting factor 1
BNIP3:	Bcl-2/ adenovirus E1B 19-kDa-interacting protein 3
CAF:	cancer associated fibroblast
CNS:	central nervous system
DAVID:	Database for Annotation, Visualization, and Integrated Discovery Analysis
ECM:	extracellular matrix
ER:	endoplasmic reticulum
ERT2:	estrogen receptor T2
FIP200:	focal adhesion kinase family interacting protein of 200-kDa
FOXO:	forkhead box O
GAS:	*Group A Streptococcus*
GcAVs:	GAS-containing autophagosome-like vacuoles

GCRMA: GC Robust Multi-array Average

GEMMs: genetically engineered mouse models

GO: gene ontology

Gy: gray

HAT: histone acteyltransferase

HDAC6: histone deactylase 6

H&E: Hematoxylin and Eosin

IACUC: Institutional Animal Care and Use Committee

iBMK: immortalized baby kidney

IL-6 interleukin-6

iMMEC: immortalized mouse mammary epithelial cells

KEAP1: Kelch-like ECH-associated protein

LC3: light chain 3

LC-MS: liquid chromatography–mass spectrometry

LIR: LC3-interacting region

m: month

MEF: mouse embryonic fibroblast

MeOH: methanol

min: minute

mTORC1: mammalian target of rapamycin multi protein complex 1

NAFLD: non-alcoholic fatty liver disease

NBR1: neighbor of BRCA1 gene 1

NCOA4: nuclear receptor coactivator 4

NDP52: nuclear dot protein 52

NF-κB: nuclear factor kappa-light-chain-enhancer of activated B cells

NRF2: NF-E2 related factor 2

OPTN: Optineurin

p62: SQSTM1; Sequestosome 1

PAS: Periodic Acid Schiff

PDAC: pancreatic ductal adenocarcinoma

PE: phosphotidylethanolamine

PI3P: phosphatidylinositol-3-phosphate

PINK1: PTEN-induced putative kinase 1; a Ser/Thr kinase

ROS: reactive oxygen species

RUBICON: RUN domain and cysteine-rich domain containing, Beclin1-interacting

SENDA: static encephalopathy of childhood with neurodegeneration in adulthood

SILAC: stable isotope labeling by/with amino acids in cell culture

SIRT1: sirtuin; silent mating type information regulation 2 homolog

TAM: Tamoxifen

TCGA: The Cancer Genome Atlas

TDCLs: tumor derived cell lines

TFEB: transcription factor EB

UBA: ubiquitin-associated

UBAN: ubiquitin binding in ABIN and NEMO

ULK:	uncoordinated-51-like kinase 1 and 2
UVRAG:	ultraviolet irradiation resistance-associated gene
VMP1:	vacuole membrane protein 1
w:	week
WAT:	white adipose tissue
WDR45:	WD repeat domain 45
WT:	wild type
ZKSCAN3:	zinc finger with KRAB and SCAN domains

CHAPTER 1

INTRODUCTION

Autophagy (from the Greek words meaning “self-eating”; auto, "self" and phagein, "to eat") is a dynamic and genetically-regulated catabolic pathway involved in the cellular turnover of proteins, organelles, and pathogens. Autophagy and proteasomal degradation are the two major cellular degradation systems. In contrast to proteasomal system, which is primarily a short-lived protein degradation system, autophagy participates in cellular remodeling and adaptation by degrading long-lived or defective proteins and organelles (Reggiori and Klionsky, 2013).

There are three types of autophagy: macroautophagy, microautophagy, and chaperon-mediated autophagy. Macroautophagy (hereafter abbreviated as autophagy) is thought to be responsible for the majority of the intracellular protein degradation in mammalian cells, by sequestering cytosolic cargo into a double membrane vesicle called autophagosome (Mathew et al., 2014; Mortimore and Poso, 1987). The autophagosome then fuses with lysosome to form an autolysosome to degrade captured material together with the membrane (Levine and Kroemer, 2008). This cellular garbage disposal mechanism maintains homeostasis under normal and pathophysiological conditions by recycling cellular components, sustaining metabolic needs by generating amino acids, nucleotides, fatty acids, sugars and increasing cellular ATP levels (Rabinowitz and White, 2010). Autophagy also sustains protein and organelle quality by eliminating protein aggregates and damaged organelles (Mizushima and Komatsu, 2011).

Autophagy is evolutionarily conserved in eukaryotes; from yeast to plants and

animals. Autophagy-deficient yeast does not survive nitrogen starvation (Tsukada and Ohsumi, 1993) and mice require autophagy during the neonatal starvation period (Kuma et al., 2004); indicating vital importance of autophagy in nutrient deprived conditions. Basal autophagy engages at a low rate in nutrient rich conditions as well, indicating the essential role of autophagy in global turnover of cellular components (Mizushima et al., 2004).

Autophagy Signaling Network

Autophagy is mainly upregulated by metabolic stresses such as hypoxia, oxidative stress, and nutrient and growth factor deprivation. During nutrient deprivation where energy is depleted, autophagy is activated to recycle intracellular substrates to replenish ATP levels. When ATP levels are low; AMPK (AMP activated protein kinase), which is an energy sensor and regulator of cellular metabolism to maintain energy homeostasis, is activated to induce autophagy. In contrast, mTORC1 (mammalian target of rapamycin multi protein complex 1), which is a nutrient-consuming anabolic process inducer, inhibits autophagy (Kim et al., 2011). PI3K/AKT and MAPK are positive regulators of mTORC1 that are activated in response to mitogens. As a result of AMPK induction, mTORC1 inhibition and/or other signals bypassing mTORC1 shown in Figure 1.1, autophagy is initiated (Fig. 1.1) (Jung et al., 2010; Mizushima and Komatsu, 2011).

Autophagy machinery proceeds in a series of distinct steps: initiation, nucleation, elongation, fusion with lysosome and degradation/recycling of cargo. These events are mainly executed by a series of autophagy-related (ATG)

proteins. A pre-initiation complex, called ULK complex, consists of ULK1/2 (uncoordinated-51-like kinase 1 and 2), ATG13, ATG101 and FIP200 (focal adhesion kinase family interacting protein of 200-kDa). ULK complex is negatively and positively regulated by phosphorylation. AMPK directly activates ULK1/2 by phosphorylating Ser317 and Ser377; on the other hand if nutrients are sufficient, mTOR induction prevents ULK1 activation by phosphorylating ULK1 Ser757 and preventing interaction between ULK1 and AMPK. (Chan, 2009; Kim et al., 2011).

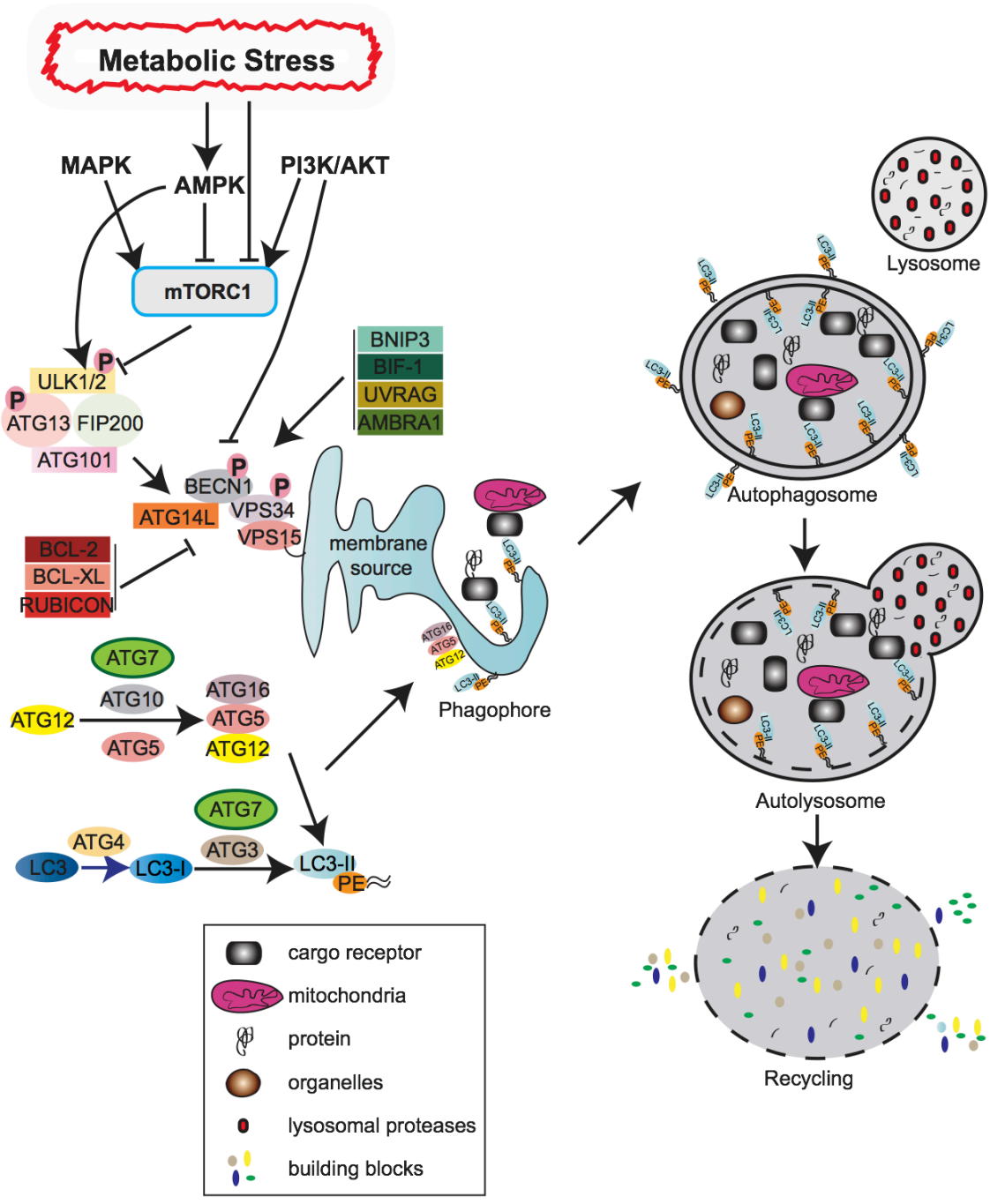

Figure 1.1 Overview of autophagy pathway.

Upon metabolic stress, AMPK phosphorylates and activates the ULK complex or AMPK suppresses mTORC1 to prevent its inhibitory effect on the ULK complex. Then the ULK complex activates the initiation complex called the Class III PI3K complex, which consists of BECN1 (BECLIN-1; BCL-2 interacting protein), ATG14L, VPS34 and VPS15. This complex is also known as nucleation complex, regarding its function to generate PI3P (phosphatidylinositol-3-phosphate) to promote autophagosomal nucleation (He and Levine, 2010; Meijer and Klionsky, 2011). VPS34 is the PI3K that is responsible for PI3P production and ATG14L specifies the VPS34 complex relocation site. AKT may directly phosphorylate BECN1 to inhibit autophagy; phosphorylated BECN1 interacts with intermediate filaments, which sequesters BECN1 from autophagy machinery. Likely, anti-apoptotic proteins BCL-2 (B-cell lymphoma 2) and BCL-XL (B-cell lymphoma extra large) indirectly regulate autophagy through suppressing the function of BECN1 by inhibiting Bax and Bak (Lindqvist and Vaux, 2014).

RUBICON (RUN domain and cysteine-rich domain containing, Beclin1-interacting) is another autophagy blocker that inhibits the function of UVRAG (ultraviolet irradiation resistance-associated gene) complex in autophagosome maturation. UVRAG and AMBRA1 (activating molecule in Beclin1-regulated autophagy) interact with BECN1 and positively regulate autophagosome formation; UVRAG also interacts with BIF-1 (Bax-interacting factor 1) to promote membrane curvature. BNIP-3 (Bcl-2/ adenovirus E1B 19-kDa-interacting protein 3), which is an atypical BH3-only protein, also acts as an autophagy inducer by interacting BECN1 (Figure 1) (Goldsmith et al., 2014; Yang and Klionsky, 2010).

In addition to these trafficking proteins, ATG9 and VMP1 (vacuole membrane protein 1) have also been associated with autophagosome membrane assembly (Yang and Klionsky, 2010). The origin of autophagosomal membrane and how it is originated is not fully understood; however, mitochondria, endoplasmic reticulum (ER) membranes, Golgi, endosome and plasma membrane are proposed to be the autophagosome membrane sources (Hamasaki et al., 2013).

Autophagosome membrane elongation and maturation require two ubiquitin-like systems. The first conjugation system involves ATG5-ATG12 conjugation that is essential for LC3 (light chain 3) lipidation. ATG7 functions like an E1-like ubiquitin activating enzyme and transfers ubiquitin-like ATG12 to ATG5. ATG12-ATG5 covalent conjugate binds ATG16 forming a multimeric complex to facilitate membrane elongation (Figure 1). In the second conjugation system, ATG7 is also responsible for LC3 conjugation with the phosphotidylethanolamine (PE) lipid, which is indispensible for LC3 to locate to the outer and inner surfaces of the autophagosome membrane. First, cysteine protease ATG4 cleaves LC3 to expose the C-terminal glycine residue (LC3-I) to which PE can bind. Then, cleaved LC3-I binds to E1-like ATG7 via a thioester bond and is transferred to E2-like ATG3 (Geng and Klionsky, 2008). Finally, LC3-I dissociates from ATG3 and associates to the amine head of PE via an amide bond (LC3-II) (Figure 1). These two ubiquitin conjugation systems are interconnected such that the ATG12-ATG5-ATG16 complex acts as an E3 ligase to determine the LC3 lipidation site while LC3 conjugation is also required for ATG12-ATG5-ATG16 multimeric complex formation (Yang and Klionsky, 2010). Interestingly, ATG4,

which is responsible for cleavage of LC3 to start its processing, is also responsible for cleavage of LC3-II to free it from autophagosome membrane (Satoo et al., 2009). All these proteins orchestrate membrane expansion resulting in autophagosome formation carrying the cargo to be degraded (Figure 1).

The next important aspect of autophagy is the identification and capture of the cargo within the autophagosome. There are a number of ubiquitin binding adaptor proteins identified as autophagy cargo receptors; including p62/SQSTM1 (Sequestosome 1), NIX, NBR1 (neighbor of BRCA1 gene 1), NDP52 (nuclear dot protein 52) and OPTN (Optineurin) (Johansen, Lamark, 2011, Wild et al, 2011). These cargo receptors have a conserved LC3-interacting region (LIR) essential for autophagosome targeting. NBR1 and p62 have UBA (ubiquitin-associated) domains, OPTN has a UBAN (ubiquitin binding in ABIN and NEMO) and zinc finger domain, NDP52 has a zinc finger domain; all these domains are involved in recognition and uptake of ubiquitinated proteins or organelles into the autolysosomes (Johansen and Lamark, 2011). OPTN and NDP52 mainly target intracellular bacteria for autophagic degradation. In addition to these cargo receptors, there are proteins like HDAC6 (histone deactylase 6), which only interacts with ubiquitin but not with LC3. HDAC6 interacts with p62; and as a result of this interaction it takes a role in aggresome formation and ensuring the cargo transport along the microtubules toward the microtubule-organizing center. NIX is a mitophagy receptor responsible for removal of mitochondria during erythrocyte differentiation, it has an LIR motif but lacks a ubiquitin binding domain; it recognizes a particular binding partner on mitochondrial outer

membrane and guarantees its delivery to the autophagosome via the LIR motif (Kirkin et al., 2009; Lippai and Low, 2014). Hence, NIX-dependent mitophagy is ubiquitin-independent. There is also a ubiquitin dependent mitophagy that involves Parkin recruitment to the mitochondria, which is a ubiquitin ligase catalyzing ubiquitin transfer to mitochondrial substrates. Initially, PINK1 (PTEN-induced putative kinase 1; a Ser/Thr kinase) recognizes depolarized mitochondria and attaches to the outer membrane. Then, it activates and recruits Parkin onto damaged mitochondria. Finally, Parkin-mediated ubiquitination results in p62 recruitment, clustering of mitochondria and mitophagy (Johansen and Lamark, 2011). Although it is not clear how, there are proteins such as ALFY and BAG3 that do not have a ubiquitin binding domain but interact with ubiquitinated proteins and autophagosomal markers (Kirkin et al., 2009). As the autophagosome forms, carrying the cargo and cargo receptors inside, it travels along microtubules and fuses to the lysosome where the acidic proteases digest and recycle the cargo (Fig. 1.1).

Regulation of Autophagy

Post-translational Regulation

Nutrients are critical autophagy regulators; autophagy is induced in nutrient starvation and this induction is predominantly controlled by mTOR and AMPK. Autophagy is strongly induced in response to glucose deprivation through BECN1/VPS34 activation by AMPK-dependent BECN1 phosphorylation (Kim et al., 2013). On the other hand, amino acids activate Rag GTPases to promote

mTORC1 translocation to the lysosome and inhibit autophagy (Sancak et al., 2010).

Activities of Atg proteins are mainly regulated by post-translational modifications such as phosphorylation (i.e. ATG13, ULK1/2, BECN1 and VPS34 phosphorylation), proteolyic cleavage and lipidation (i.e. LC3 cleavage and lipidation with PE) as mentioned in detail in the previous section. Moreover, oxidation and acetylation also modulate the function of Atg proteins. Under starvation conditions, reactive oxygen species (ROS) -specifically hydrogen peroxide- formation is stimulated and ATG4 is directly oxidized and activated by hydrogen peroxide (Scherz-Shouval et al., 2007). Recent studies have also reported that, SIRT1 (sirtuin; silent mating type information regulation 2 homolog), mammalian deacetylase, is important for autophagy activation. ATG5, ATG7 and ATG8 are acetylated in normal conditions; SIRT1 directly interacts and deacetylates these proteins to induce autophagosome formation during starvation (Lee et al., 2008).

Transcriptional Regulation

Autophagy is transcriptionally regulated in addition to post-translational modifications. One example is the evolutionarily conserved FOXO (forkhead box O) transcription factors; they translocate between nucleus and cytoplasm in response to phosphorylation. FOXO transcription factors are autophagy inducers in both nuclear (transcriptional) and cytoplasmic (transcription-independent) locations. In response to stress, FOXO proteins are phosphorylated by AKT1 and shuttle to the nucleus to transcriptionally upregulate *Atg* genes in hepatocytes,

cardiomyocytes, neurons and primary renal proximal tubular cells (Webb and Brunet, 2014).

E2F1 is another autophagy transcription factor, which directly binds to the hypoxia inducible-death factor *Bnip3* promoter to activate autophagy in hypoxic conditions. E2F1 also transcriptionally activates *LC3*, *ULK1* and *ATG5*. NF-κB (nuclear factor kappa-light-chain-enhancer of activated B cells) is involved in BNIP3 regulation as well and acts as a molecular switch by binding to the *Bnip3* promoter to occupy and repress its activation in normal conditions. On the other hand, NF-κB is an autophagy activator, which induces *BECN1*, *BCL2* and *p62* expression by binding to their antioxidant response elements (AREs) in the promoter region (Jain et al., 2010; Niture and Jaiswal, 2012; Wruck et al., 2011).

The autophagy process depends on cooperation of autophagosomes and lysosomes. There are also transcription factors that are involved in regulation of autophagosome and lysosome biogenesis. Transcription factor EB (TFEB) functions as a transcriptional activator (e.g.: activates *WIPI*, *p62* and *UVRAG*) and ZKSCAN3 (zinc finger with KRAB and SCAN domains) functions as a repressor (e.g.: represses *LC3*, *WIPI* and *ULK1*) (Settembre et al., 2011).

p53, ‘the guardian of genome’, conserves cellular stability by regulating expression of stress response genes activated in response to hypoxia, DNA damage and cell cycle abnormalities. Consistent with its function, p53 is just as involved in autophagy regulation as it is involved in other biological processes. But it is a double-edged sword by means of its changing role dependent on its subcellular localization. Nuclear p53 inhibits mTOR and in turn promotes

autophagy (Feng et al., 2005); however cytoplasmic p53 is claimed to inhibit autophagy although the mechanism is unknown (Tasdemir et al., 2008).

Epigenetic and miRNA-dependent Regulation

Histone modifying enzymes have been implicated in regulating autophagy. Interestingly, a nuclear role of histone acteyltransferases (HATs) and histone deacetylases (HDACs) in regulating autophagy has not been experimentally shown. HDAC inhibitors have cell-type specific effects: HDAC inhibitors are autophagy inducers in yeast, mouse embryonic fibroblasts (MEFs), skeletal muscle cells and some cancer cells including HeLa and glioblastoma; but they are autophagy repressors in cardiomyocytes (Fullgrabe et al., 2014). HATs are counterparts of HDACs that are involved in autophagy regulation. Esa1, which is a yeast HAT, acetylates Atg3 and induces autophagy (Fullgrabe et al., 2014; Yi et al., 2012).

MicroRNAs, as in other biological processes like proliferation, differentiation and apoptosis, have emerged as important regulators of autophagy genes, starting from initiation to elongation. To date the main targets of microRNAs are: ULK1/2 in initiation; BECN1 and UVRAG in nucleation; ATG4, ATG5, ATG7, ATG10, ATG12, ATG16, BNIP3, LC3 and p62 in elongation. Despite the computationally identified set of microRNAs, currently there are no microRNAs experimentally confirmed to regulate the fusion step. In addition, autophagy, in turn, regulates expression of several microRNAs (Frankel and Lund, 2012; Fullgrabe et al., 2014).

Physiological Functions of Autophagy

Autophagy, as a cellular housekeeper, functions for quality control of intracellular proteins and organelles integrity. In normal conditions, basal autophagy maintains cellular homeostasis by degrading and recycling unfolded and superfluous proteins. When properly regulated, this disposal mechanism maintains homeostasis under normal and pathophysiological conditions by removing toxic waste, recycling cellular components, sustaining metabolic needs by generating amino acids, nucleotides, fatty acids, sugars, and increasing cellular ATP levels (Rabinowitz and White, 2010). However, in response to stress or during differentiation (e.g. embryogenesis and maturating erythrocytes), some organelles and proteins are selectively disposed and recycled; such as selective autophagic removal of mitochondria (mitophagy), peroxisomes (pexophagy), ER (reticulophagy), ribosomes (ribophagy), intracellular pathogens as bacteria and virus (xenophagy), and protein aggregates caused by the presence of aggregation-prone often mutant or misfolded proteins (aggrephagy) (Johansen and Lamark, 2011). In addition to eliminating unwanted or toxic material, selective autophagy removes potential sources of ROS by mitophagy and pexophagy. Autophagy deficiency in skeletal muscle and mutations in *Atg1* causes accumulation of mitochondria and peroxisomes, respectively; which in turn increases ROS levels (Manjithaya et al., 2010; Masiero et al., 2009).

Increase in ROS activates anti-oxidant defense, which is regulated by NRF2 (NF-E2 related factor 2), a transcription factor involved in regulation of transcriptional control of antioxidant and detoxifying genes. In quiescent

conditions, NRF2 is degraded by an E3 ligase, called KEAP1 (Kelch-like ECH-associated protein 1). KEAP1 also interacts with p62; hence, p62 accumulation will sequester KEAP1, resulting in NRF2 nuclear translocation and expression of its target genes (Komatsu et al., 2010). Therefore, although the molecular mechanism of this interplay is not clearly known, p62 is indirectly involved in cellular antioxidant response through NRF2.

A newly discovered role for autophagy is for the regulation of bioavailable iron. This process manages the autophagic turnover of ferritin (ferritinophagy) by which the autophagy receptor NCOA4 (nuclear receptor coactivator 4) recognizes the iron complex to be recycled and maintains iron homeostasis (Mancias et al., 2014).

Autophagy also functions in regulating intracellular lipid storage by breaking down triglycerides and cholesterol stored in lipid droplets; this process is called lipophagy. Lipophagy by itself is a representative example for the physiological relevance of autophagy in energetic balance when we consider high energy density of fat stores. Impaired autophagy in liver causes hepatic lipid droplet accumulation; in addition to that, fibroblasts, neurons and stellate cells also require autophagy for lipid breakdown (Liu and Czaja, 2013). Lipophagy levels vary in response to the extracellular supply of nutrients. For example, free fatty acids and high-fat diet reduces lipophagy through feedback inhibition (Singh et al., 2009a).

On the other hand, autophagy has a distinct role in regulating adipose lipid physiology. Instead of breaking down lipids, autophagy is required to maintain

large lipid droplets and fat mass in adipose tissue. Adipocyte-specific *Atg7* knockout mice have reduced white adipose tissue (WAT) and increased brown adipose tissue (BAT); and the mice are lean and resistant to high fat diet-induced obesity (Singh et al., 2009a; Zhang et al., 2009).

Given the role of autophagy in quality control of cellular homeostasis and in maintenance of the cellular energetic balance, not surprisingly, dysregulation of autophagy is associated with a broad spectrum of multi-systemic and metabolic disorders. For example, metabolic disorders such as diabetes and obesity are the phenotypic illustrations of a loss in energy homeostasis, which has been correlated with altered autophagy. In genetic and dietary models of obesity, hepatocytic autophagy is observed to be downregulated. Furthermore, defective autophagy in liver compromises insulin signaling and defective autophagy in adipose induces high fat diet dependent obesity and increases insulin sensitivity (Yang et al., 2010; Zhang et al., 2009).

Aging is closely associated with accumulation of proteins, organelles (mostly mitochondria) and ROS; the more the cells accumulate damaged substrates, the more they age. Caloric restriction extends lifespan; this effect is directly correlated with autophagy induction. Longevity-promoting effects of the caloric restriction is blocked by autophagy ablation (Rubinsztein et al., 2011). Additionally, rapamycin, a pharmacological inhibitor of mTOR that suppresses autophagy, extends the lifespan of yeast, fruit flies and mice; which is possibly through autophagy activation (Alvers et al., 2009; Bjedov et al., 2010; Harrison et al., 2009). However, a recent study on mice showed that lifespan extension is not

due to modulation of aging since similar effects were also observed in young mice (Neff et al., 2013).

Recent studies have shown that dysregulation of autophagy might contribute organ specific diseases (Fig. 1.2). Mutations, polymorphisms, haplo-insufficiencies, dysfunctional adaptor proteins or the reduced ability to recognize the cargo by the autophagy receptors p62 and NBR1 are the main underlying causes of altered autophagy in diseases. Autophagy acts as a protective mechanism against various pathophysiological conditions mainly due to its role in clearance of p62-positive accumulated organelles and proteins essentially in post-mitotic tissues as neurons and cardiomyocytes. Neurons cannot dilute their waste burden by cell division and therefore rely highly on autophagy to prevent accumulation of cellular waste. As neurons age they become more sensitive to slowdown in autophagic clearance and they tend to degenerate by accumulating more waste. Parkinson's disease, Alzheimer's disease and Huntington's disease have increased levels of accumulated protein inclusions and aggregates, possibly due to defective protein/organelle clearance. (Rubinsztein et al., 2012).

It has been shown that autophagy is important in the intracellular clearance of α-synuclein, a characteristic Parkinson Disease component of neuronal cytoplasmic inclusions (Lewy bodies) (Webb et al., 2003). In addition to these, defective mitochondria turnover by mitophagy and lysosomal disorders are found to be exceptionally linked to neurodegenerative diseases (Nixon, 2013). Mutations in p62 are found to be directly associated with amyotrophic lateral sclerosis (Rea et al., 2014). Very recently, Saitsu et al. identified *de novo*

mutations in an autophagy related gene, WDR45 (WD repeat domain 45), cause neurodegenerative disease called static encephalopathy of childhood with neurodegeneration in adulthood (SENDA) by whole-exome sequencing (Saitsu et al., 2013).

Other than neurodegenaration, increasing evidence suggests that autophagy defects are associated with cardiovascular disorders such as cardiomyopathy, ischemia, congestive heart failure and Danon disease. Accumulated autophagosomes were detected in myocardial biopsy samples from cardiovascular patients (Terman and Brunk, 2005).

Other organ-specific diseases with altered autophagy such as cystic fibrosis, muscle and liver disorders are mostly based on decreased clearance of aggresomes causing abnormal accumulation of defective organelles, proteins and lipids (Fig. 1.2) (Schneider and Cuervo, 2014).

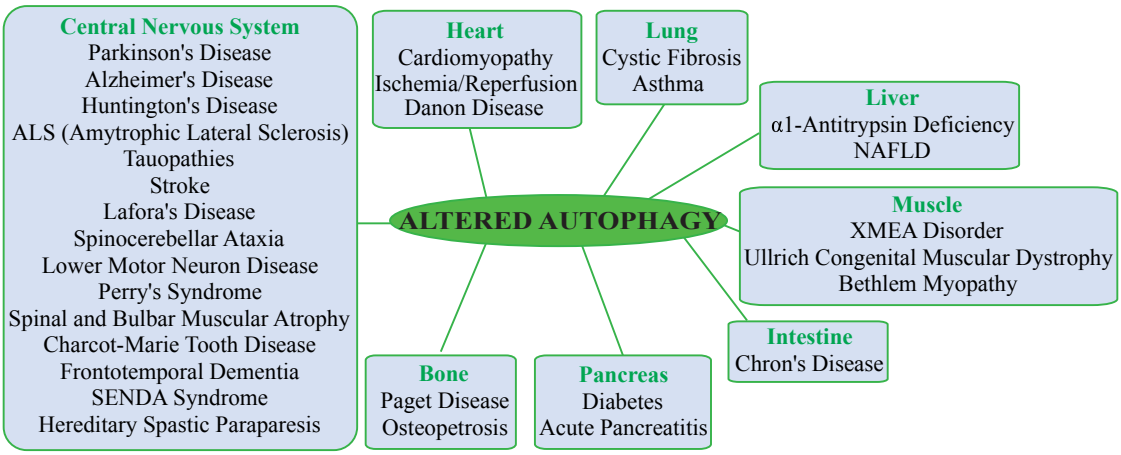

Figure 1.2 Organ specific human diseases with altered autophagy

Autophagy has also emerged as a regulator of differentiation and development. In addition to modulating adipogenesis as mentioned above, autophagy is also essential for preimplantation development, erythrocyte and lymphocyte differentiation. The very initial autophagic events in mammalian development appear in fertilized oocytes, which are dependent on ATG5 function (Tsukamoto et al., 2008). Following fertilization, except for the brain, autophagy levels profoundly increase in all tissues to degrade maternal mRNA and proteins (Kuma et al., 2004). Afterwards the protein synthesis encoded by a zygotic embryo is initiated. Autophagy is upregulated in the neonatal period in response to severe starvation. Consistently, knockouts of *Atg3*, *Atg5*, *Atg7*, *Atg9*, and *Atg16L1* cause neonatal lethality. The absence of several upstream regulators display more severe phenotypes, such as *Beclin1*, *Ambra1*, and *FIP200* deficiency inducing embryonic lethality likely due to autophagy-independent functions (Mizushima and Levine, 2010).

Additionally, autophagy is essential for erythrocyte and lymphocyte differentiaton mainly through NIX-dependent mitochondrial clearance. During lymphocyte differentiation, autophagy deficiency reduces T and B lymphocyte counts. In addition to mitochondrial accumulation, lymphocytes tend to increase superoxide and sensitivity to apoptosis when autophagy is ablated (Mortensen et al., 2010; Novak et al., 2010).

Autophagy and cancer

Autophagy has a context dependent role in cancer; on the one hand, as a stress response mechanism, autophagy prevents cellular and tissue damage that can promote cancer initiation. On the other hand, as a survival and fitness mechanism for tumor cells, especially in hypoxic regions, autophagy maintains the energy homeostasis required for tumor survival and growth (White, 2012). Understanding the functional role of autophagy in cancer and other diseases is important to rule out possible therapeutic implications.

Autophagy as a tumor suppressor

Autophagy guards the cell by removing damaged organelles, preventing excess ROS, suppressing DNA damage and by maintaining genome stability (Mathew et al., 2007). Initial studies have shown that mice with heterozygous loss of BECN1 have an increased incidence of spontaneous tumors (Qu et al., 2003). Moreover, BECN1 heterozygous-deficient immortalized baby kidney (iBMK) cells and mouse mammary epithelial cells (iMMECs) display more tumorigenic characteristics than wild type (WT) cells (Karantza-Wadsworth et al., 2007; Mathew et al., 2007). BECN1 was previously proposed to be a

haploinsufficient tumor suppressor in breast, ovarian and prostate cancers (Aita et al., 1999); however, a recent study analyzing human cancer sequencing data from 10,000 tumors and matched normal tissues in The Cancer Genome Atlas (TCGA) showed that there was no evidence for selective *BECN1* mutation or loss in any human cancers. Although large deletions encompassing both *BRCA1* and *BECN1* together were detected in breast and ovarian cancers probably due to their adjacent locations on the same chromosome, there were no significant deletions or mutations in only *BECN1*. (Laddha et al., 2014).

In addition to these observations, mice with mosaic deletion of *Atg5* or liver specific deletion of *Atg7* develop multiple spontaneous benign liver hepatomas due to accumulation of p62. This suggests that the tumor-suppressor function of autophagy is liver-specific. (Takamura et al., 2011). Autophagy also indirectly suppresses tumorigenesis; tumor suppressor genes, such as *PTEN*, *LKB1*, *p53*, *TSC1* and *TSC2*, can induce autophagy via inhibiting mTOR (Rubinsztein et al., 2012). But whether these tumor-promoting functions of autophagy occur in human cancers has yet to be determined.

Autophagy as a tumor promoter

With tumor progression, cancer cells face metabolic crisis in response to nutrient and growth factor deprivation specifically in hypoxic regions due to insufficient vascularization. Under these conditions, autophagy helps cancer cells by sustaining their nutrient availability and energy balance through recycling autophagic substrates (Degenhardt et al., 2006). Consistent with this idea, RAS-driven tumor cells activate autophagy and are highly dependent on autophagy to

survive starvation, mainly through maintaining mitochondrial function. Autophagy deficiency also impairs the tumorigenecity of RAS-driven cancer cells. RAS-transformed cells with defective autophagy have reduced levels of mitochondrial oxygen consumption and TCA cycle intermediates (Guo et al., 2011; Yang et al., 2011). Not only limited to the RAS oncogene, inhibiting autophagy by pharmacological inhibitors or by RNA interference to silence *Becn1*, *Atg5*, *Atg10* or *Atg12* also accelerates the death of starved cancer cells (Boya et al., 2005). Additionally, deficiency in the essential autophagy gene *Fip200* in the polyoma middle T mouse mammary cancer model compromised tumor growth (Wei et al., 2011).

Autophagy is also essential in proteome remodeling in cancer cells. A recent SILAC (stable isotope labeling by/with amino acids in cell culture) study by comparing the global proteome of autophagy-functional and -deficient RAS-driven cancer cells showed that autophagy selectively recycles proteins in non-essential pathways and proinflammatory signaling, but preserves vesicle trafficking, autophagic and stress survival proteins; indicating the importance of autophagy in tumor survival (Mathew et al., 2014).

With recent studies, genetically engineered mouse models (GEMMs) for lung and pancreatic cancer provided supporting evidence for how autophagy promotes tumor growth. Tumor-specific deletion of *Atg5* or *Atg7* in $KRAS^{G12D}$-induced GEMM of lung cancer suppressed cell proliferation and reduced tumor burden. More interestingly, autophagy ablation within the tumor changed morphology of tumor cells into a benign state, remarkably, autophagy-deficient

tumors displayed oncocytic differentiation, marked by the accumulation of respiration defective mitochondria. Additionally, autophagy deficiency also increased p53 induction in KRAS-driven tumors, suggesting that autophagy is required to limit p53 function to promote tumor growth. However, in the absence of p53, autophagy ablation still impairs KRAS-driven tumor growth, which might be through defective lipid metabolism (Guo et al., 2013a; Rao et al., 2014). Autophagy is also required for mammary tumorigenesis, and monoallelic loss of BECN1 impaired PALB2-associated mammary tumorigenesis (Huo et al., 2013).

$BRAF^{V600E}$-driven lung cancer also requires ATG7 for tumor progression (Strohecker et al., 2013). Interestingly, in the BRAF-driven GEMM of lung cancer, ATG7 depletion initially promoted tumor progression due to an induction in oxidative stress, similar to NRF2 deficiency. However, over time, ATG7 deficiency resulted in defective mitochondria accumulation, reduced tumor burden and oncocytic change as observed in KRAS-driven GEMM of lung cancer (Guo et al., 2013a; Strohecker et al., 2013). *In vitro* studies using tumor cells derived from KRAS- or BRAF-driven lung cancers showed that Atg7-deficient tumor cells have impaired mitochondrial respiration. Autophagy ablated tumor cells are sensitive to starvation-induced death, which can be rescued by glutamine supplementation, indicating the reason for autophagy addiction of cancer cells might be to sustain mitochondrial function and glutamine metabolism (Guo et al., 2013a; Strohecker et al., 2013).

Similarly, when p53 is inactivated by somatic loss of heterozygosity (similar to human tumors) in a RAS-driven pancreas GEMM, autophagy deficiency inhibited

pancreatic ductal adenocarcinoma (PDAC) progression (Yang et al., 2014). In contrast, according to another study, autophagy inactivation in a PDAC mouse model only inhibited tumor growth when p53 was present. However, in this model both alleles of *p53* were deleted during embryogenesis (Rosenfeldt et al., 2013), which is irrelevant in human PDAC (Yang et al., 2014). Therefore, as in lung cancer models, autophagy ablation impairs PDAC tumor progression irrespective of p53 status.

$BRAF^{V600E}$ mutation is also observed in pediatric central nervous system (CNS) tumors, and BRAF-driven CNS tumor cells have high levels of autophagy and are sensitive to pharmacologic and genetic autophagy suppression. Furthermore, chloroquine treatment increases the sensitivity to the BRAF inhibitor vemurafenib (Levy et al., 2014).

In addition to autophagy induction in tumor cells, surrounding stromal cells in the nutrient deprived and stressed environment also upregulate autophagy to stimulate tumor growth. A striking example comes from cancer associated fibroblasts (CAFs): these cells promote autophagy/mitophagy and recycle metabolites as amino acids, ketone bodies and glycolytic intermediates to support the growth and aggressiveness of adjacent tumor cells. Specifically, mitophagy in CAFs accelerates aerobic glycolysis and drives the secretion of high-energy metabolites such as lactate and pyruvate (Martinez-Outschoorn et al., 2010; Salem et al., 2012).

Autophagy also provides support for cellular invasion and metastasis for tumor cells. For example, the invasion of autophagy deficient RAS-transformed

epithelial cells is impaired in 3D culture due to insufficient secretion of invasion factors, such as the promigratory cytokine interleukin-6 (IL-6). Consistently, these autophagy-deficient cells are not dynamic enough to induce pulmonary metastasis in mammary, lung and hepatocellular carcinoma (Lock et al., 2014; Peng et al., 2013). One possible role for autophagy in metastasis might be enabling survival to through extracellular matrix (ECM) detachment, because RAS-driven human cancer cell lines upregulate autophagy during detachment. Autophagy suppression impairs adhesion-independent growth of RAS-transformed cells (Fung et al., 2008). Also, cells with ablated autophagy have low levels of matrix metalloproteinase 2 and WNT5A (Lock et al., 2014).

Autophagy in Host Defense

Studies in recent years have firmly established that autophagy acts in an immune response pathway targeting intracellular pathogens such as bacteria and viruses (xenophagy). After invading host cells, the bacterium populates in the vacuole or phagosome, or it may even damage the membrane and escape into the cytosol. Then the host cells recognize the bacteria to recruit them through autophagy to lysosomal degradation. For example, autophagy targets *M. tuberculosis* within vacuolar membranous compartments and a recent study showed that 30% of mycobacteria are selectively targeted by LC3 and ATG12 immediately after infection (Watson et al., 2012).

Group A Streptococcus (GAS) is another example of an autophagy targeted bacterium, which is cytosolic. It has a toxin called streptolysin O, which facilitates its escape from endosomes to the cytoplasm. It is recognized by this toxin and is

trapped in GAS-containing autophagosome-like vacuoles (GcAVs) to be degraded by autophagy. ATG5-deficient mouse embryonic fibroblasts have impaired GcAV formation and reduced bacterial clearance, supporting the importance of autophagy in host defense (Nakagawa et al., 2004).

Furthermore, *S. Typhimurium* is recognized and recruited to the autophagosome by p62 and *Salmonella* is targeted by NDP52; which indicates the importance of cargo receptors for efficient targeting and killing of pathogens (Cemma et al., 2011; Zheng et al., 2009). BECN1 overexpression also prevents replication of Sindbis virus, suggesting a role for autophagy against viral infection (Liang et al., 1998).

In contrast, autophagy may help some pathogens in invasion and escape from host defense responses. *P. gingivalis* and *B. abortus* reside in autophagosomal vacuoles. Upon infection, they localize into early endosome-like vacuoles and afterwards autophagosomes, preventing autophagosome fusion with lysosome and lysosomal degradation (Dorn et al., 2002).

CHAPTER 2

MATERIALS AND METHODS

Mice

All animal care and treatments were carried out in compliance with Institutional Animal Care and Use Committee (IACUC) guidelines. *Ubc-CreERT2* mice (Ruzankina et al., 2007) (Jackson Laboratory, Bar Harbor, ME) and *Atg7*$^{flox/flox}$ mice (Komatsu et al., 2005) (provided by Dr. M. Komatsu, Tokyo Metropolitan Institute of Medical Science) were cross-bred to generate *Ubc-CreERT2/*$^{+}$*;Atg7*$^{flox/flox}$ mice. Compound *Ubc-CreERT2/*$^{+}$*;Atg7*$^{flox/flox}$ mice were also bred to *Trp53*$^{flox/flox}$ (Jackson Laboratory, Bar Harbor, ME) mice to generate *Ubc-CreERT2/*$^{+}$*;Atg7*$^{flox/flox}$*;Trp53*$^{flox/flox}$ mice.

To acutely delete *Atg7* throughout the mouse we used the Cre-ERT2 transgenic system where expression of the Cre recombinase-ERT2 fusion protein is under transcriptional control of a ubiquitous promoter (*Ubc*) and is activated by Tamoxifen (TAM) interaction with the ERT2 (estrogen receptor T2) domain. TAM (Sigma, T5648) was suspended at a concentration of 20 mg/ml, in a mixture of 98% sunflower seed oil (VWR, 700011-932) and 2% ethanol and 200 µl per 25 g of body weight and was injected intraperitoneally into 8 to 10 week old male and female *Ubc-CreERT2/*$^{+}$*;Atg7*$^{flox/flox}$ and *Ubc-CreERT2/*$^{+}$*;Atg7*$^{flox/flox}$*;Trp53*$^{flox/flox}$ mice once per day for 5 days and tissues were analyzed at indicated times following the last day of TAM administration. *Atg7*$^{flox/flox}$ (control group) received the same amount of TAM, but did not express the CreERT2 fusion protein and *Ubc-CreERT2/*$^{+}$ (control group) received the same amount of TAM to assess and exclude Cre specific affects.

To assess the consequence of acute *Atg7* deletion in response to fasting, 10

days following the last day of 5-day TAM administration, mice were fasted for 24 hours with free access to water but no food. At 20-24 hours post fasting, plasma was collected for hormonal and, biochemical analysis and tissues were harvested for histological examination. For glucose supplementation, mice were provided drinking water containing 10% glucose throughout fasting.

To assess the consequence of acute ATG7 deletion to tumorigenesis, compound *Ubc-CreERT2;Atg7* mice were bred to *FSF-Kras*^{G12D} mice (Young et al., 2011) (Jackson Laboratory, Bar Harbor, ME) and *Trp53*$^{frt/frt}$ mice (Singh et al., 2010) (provided by Dr. L. Johnson, Genentech) to generate *Ubc-CreERT2*$^{-/+}$*;Kras*$^{G12D\text{-}frt/+}$*;p53*$^{frt/frt}$*;Atg7*$^{+/+}$ and *Ubc-CreERT2*$^{-/+}$*;Kras*$^{G12Dfrt/+}$*; p53*$^{frt/frt}$*;Atg7*$^{flox/flox}$ mice. To activate RAS and delete *p53* in the lung and produce tumors, mice were infected intranasally with recombinant, replication-deficient adenovirus expressing Flp recombinase (Ad-FlpO, University of Iowa Adenoviral Core, Iowa City, IA) at 1.2 x 10^8 pfu/mouse at 6-8 weeks of age.

EchoMRI and micro-CT

To measure body composition, fed or fasted living mice with and without *Atg7* (*Atg7*$^{\Delta/\Delta}$) were imaged by EchoMRI (Echo Medical System) to obtain fat and lean mass measurements. To monitor lung tumor burden *in vivo* mice were anesthetized using isofluorane. Respiratory gated and low resolution CT images of maximally ventilated mice were acquired using a Siemens Inveon PET/CT. Reconstructed data were processed through a Gaussian filter by using INVEON Research Workplace software and pulmonary tissue was determined and segmented and its volume was calculated. Three-dimensional reconstructed

pulmonary images and transverse sections were generated using Osirix software.

Mouse Irradiation

At 10 days post-TAM, mice were irradiated with 10 Gy from a ^{137}Cesium source (Gammacell 40 Exactor) at a dose rate of 0.97Gy/min, and monitored daily.

Gene expression analysis

Liver and muscle tissues were snap-frozen for RNA extraction. Extracted RNAs were processed, labeled and hybridized to the Affymetrix GeneChip Mouse Genome 430A 2.0 array. The raw Affymetrix CEL files for liver and muscle samples were analyzed with Agilent GeneSpring GX11 software. Quality control was performed to remove bad quality probes. Normalized expression values were calculated by the GC Robust Multi-array Average (GCRMA) algorithm and subjected to mean transformation to collapsed all probe sets to respective genes in R. Collapsed gene expression values from all samples were used to find differentially expressed genes. The average of the two replicates for each category was calculated and 10 days post-TAM-treated fed and fasted, *Atg7*$^{flox/flox}$ or *Atg7*$^{\Delta/\Delta}$ adult mice gene expression levels were compared to find the differentially expressed genes for respective tissue samples. We used fold change threshold of 3 to call genes to be significantly changed in each category. We did not use p-values because there are only two replicates for each category. The differentially expressed genes were then used to identify enriched biological process using the Database for Annotation, Visualization, and Integrated

Discovery Analysis (DAVID 6.7) (Huang et al., 2009). Enriched Gene Ontology (GO) terms for the differentially expressed genes were examined and significant GO biological processes with Bonferroni corrected p-value less than 0.05 were plotted. We took the union of differentially expressed genes from each comparison and plotted heatmaps relative to fed *Atg7*$^{flox/flox}$ mice samples. Genes that are known to play direct or indirect role for gluconeogenesis, atrophy and autophagy were selected manually from the union of differentially expressed gene list and heatmaps were plotted.

Serum assays

Blood glucose was measured with a True2Go glucose meter (Nipro Diagnostics). Serum insulin and leptin levels were determined with ultra sensitive mouse insulin (Crystal Chem Inc., 90080) and leptin (Crystal Chem Inc., 90030) ELISA kits. Serum free fatty acids (FFAs) and β-hydroxybutyrate were measured using commercial kits from Cayman Chemical (700310 and 700190, respectively). Serum AST and ALT levels were determined using Olympus AU2700 (Idexx Bioresearch, West Sacramento, CA).

Metabolomic analysis by LC-MS

Samples were analyzed by liquid chromatography–mass spectrometry (LC-MS), which involved reversed-phase ion-pairing chromatography coupled by negative mode electrospray ionization to a stand-alone orbitrap mass spectrometer (Thermo Scientific). For serum metabolite analysis, 200 µl of cold methanol was added to 30 µl of serum, vortexed and kept at -20°C for 20 min, then centrifuged for 10 min at 13000 rpm at 4°C. Insoluble pellets were

resuspended in 1000 µl 40:40:20 methanol:acetonitrile:water, vortexed and kept on ice for 10 min, then centrifuged for 10 min at 13000 rpm at 4°C. Supernatants from two rounds were combined and dried under N_2, and reconstituted in LC-MS grade water. LC-MS was operated in negative full-scan mode at 1 Hz at 100,000 resolution with LC separation on a Synergy Hydro-RP column (100 mm X 2 mm, 2.5 µm particle size, Phenomenex, Torrance, CA) using a gradient of solvent A (97:3 H_2O/MeOH with 10 mM tributylamine and 15 mM acetic acid), and solvent B (100% MeOH). Peak intensity data was further analyzed using Excel and MatLab.

Tumor burden quantification

Hematoxylin and Eosin (H&E) stained whole slide lung tissues were scanned at 40X magnification using a Leica SCN-400 scanner (Histowiz, Brooklyn, NY). To measure tumor burden, a segmentation protocol was used which is implemented and run with Matlab. Within this protocol, tumor masks and whole tissue masks were computed from slide images by using image-processing operators. These segmented masks were used to compute tumor burden ratios.

Tumor transplantation experiment

At 10 days post-TAM, tumor derived cell lines (TDCLs) from *Atg7*-intact tumors (Guo et al., 2013a) were subcutaneously injected into *Atg7* intact or $Atg7^{\Delta/\Delta}$ mice. 10^6 cells/injection and two injections were performed on each mouse and tumor growth was monitored. Mice were sacrificed at 3.5 weeks post-injection and 5 weeks post-TAM and tumors were dissected and fixed with paraffin for histology.

Electron microscopy

Lung tumors were fixed in 0.1 M cacodylate buffer (pH 7.4) with 2.5% glutaraldehyde, 4% paraformaldehyde, and 8 mM $CaCl_2$. Fixed samples were processed as described previously (Guo et al., 2011) and images were captured with an AMT XR41 digital camera at 80 Kv on a JEOL 1200EX transmission electron microscope.

Histology

Mouse tissues were fixed in 10% buffered formalin solution (Formalde-Fresh, Fisher Scientific, SF94-4). Lung lobes were fixed for 4 hours, and all other tissues were fixed overnight. Fixed tissues were then transferred to 70% ethanol for paraffin-embedded sections. For frozen sections, tissues were fixed in 10% buffered formalin solution for same amount of time as paraffin-embedded sections, then transferred to 15% sucrose for 2 hours and transferred to 30% sucrose overnight before processing.

For immunohistochemistry, paraffin-embedded sections were stained with antibodies against ATG7 (Sigma, A2856; Santa Cruz, sc-33211), p53 (Leica, NCL-p53-505) LC3 (Nano Tools, LC3-5F10), p62 (Enzo Life Sciences, PW9860-0100), active CASPASE-3 (Cell Signaling, 9661), TOM20 (Santa Cruz, sc-11415), KI67 (Abcam, ab-15580), S6 ribosomal protein (Cell Signaling, 2217), p-S6 ribosomal protein (Cell Signaling, 4858), 4E-BP1 (Cell Signaling, 9644), p-4E-BP1 (Cell Signaling, 2855), ERK (p44/42 MAPK) (Cell Signaling, 9102), p-ERK (p-p44/42 MAPK) (Cell Signaling, 4376) and γ-H2AX (Cell Signaling, 2577). Paraffin embedded liver tissue sections were used for Periodic Acid Schiff (PAS)

staining (Sigma, 395B-1KT). For quantification of IHC for KI67 and Active CASPASE-3, the most representative whole lung lobe was analyzed by quantifying at least 20 images at 100X magnification. A minimum of 150 cells from each image were scored for each genotype. Statistical significance was calculated by two-way ANOVA with Bonferroni post-test.

Western blotting

Tissues and tumor samples were ground in liquid nitrogen and lysed in Tris lysis buffer (1 M Tris HCl, 1 M NaCl, 0.1 M EDTA, 10% NP40), and probed with antibodies against ATG7 (Sigma, A2856), LC3 (Novus Biologicals, NB600-1384), p62 (Guo et al., 2011), active CASPASE-3 (Cell Signaling, 9661) and β-ACTIN (Sigma, A1978).

Oil red O staining

Fixed frozen tissue sections were stained with pre-warmed Oil red O solution (0.5g Oil red O in 100ml Propylene glycol) for 10 min in a 60°C oven, then differentiated in 85% propylene glycol solution for 1min and rinsed with distilled water twice, then counterstained with hematoxylin lightly, rinsed with distilled water and mounted.

Bacterial analysis

Bacterial analysis was performed on biological samples. Urine and vaginal discharge were collected and incubated in commercial 5% sheep blood agar at 35°C in a 7% CO_2 incubator up to 48 hours. Individual colony types were

identified using the Bruker Biotyper MALDI-TOF spectrometer (Idexx Bioresearch, Columbia, MO).

CHAPTER 3

AUTOPHAGY IS REQUIRED FOR GLUCOSE HOMEOSTASIS AND STRESS SURVIVAL

Summary

Autophagy, a catabolic survival mechanism, captures and degrades proteins and organelles for cellular recycling to support metabolism. Meanwhile, autophagy is also essential for protein and organelle quality control. Mice constitutively deficient in autophagy essential genes, *Atg5* or *Atg7*, die within one day after birth due to amino acid deprivation during the neonatal starvation period even when force-fed. Accordingly, autophagy is required to maintain serum amino acid levels to prevent metabolic crisis in newborn mice. In order to understand the functional consequence of systemic autophagy inactivation in adult mice, we generated a mouse model where *Atg7* could be deleted conditionally and systemically in adult mice. In contrast to neonates, autophagy is dispensable for the survival of adult mice in the short term. Acute and systemic loss of ATG7 in adult mice surprisingly showed little toxicity for 5 weeks; however, autophagy ablation was detrimental within 2-3 months due to susceptibility to infection and neurodegeneration. Then, we addressed the role of autophagy during starvation. When autophagy deficient adult mice are fasted; they suffered from cachexia and died of hypoglycemia, which is mediated by p53. Moreover, we found that *Atg7* deficiency increases sensitivity to γ-irradiation induced death. These findings reveal for the first time how autophagy supports systemic metabolism and stress survival in the setting of an adult mammal.

Introduction

Mice constitutively deficient in *Atg5* or *Atg7* are born developmentally normal but fail to survive the neonatal starvation period due to metabolic insufficiency, illustrating the importance of autophagy to supply metabolic substrates to bridge gaps in nutrient availability (Komatsu et al., 2005; Kuma et al., 2004). Neuronal-specific deficiency in *Atg5* or *Atg7* results in the accumulation of autophagy substrates such as aggregated and ubiquitinated proteins and damaged organelles, motor and behavioral defects, neurodegeneration, and lethality between 1-6 months after birth (Hara et al., 2006; Komatsu et al., 2006). These findings suggest that autophagy is critical for preventing the toxic accumulation of damaged proteins and organelles in post-mitotic tissues, although there is a potential additional contribution of autophagy to brain energy metabolism.

Mosaic or liver-specific deletion of *Atg5* or liver-specific deficiency in *Atg7* also causes accumulation of autophagy substrates, hepatomegaly, hepatic cell swelling and eventual hepatoma development, suggesting that autophagy prevents liver damage and limits liver cancer initiation (Komatsu et al., 2005; Ni et al., 2012; Takamura et al., 2011). Likely, muscle specific autophagy inhibition causes myofiber degeneration and muscle weakness (Masiero et al., 2009). Additionally, defective autophagy in adipose tissue directly effects adipose mass and differentiation (Singh et al., 2009b; Zhang et al., 2009). Additional tissue-specific knockout studies underscore the importance of autophagy in tissue homeostasis, metabolism, and stem cell maintenance (Mizushima and Komatsu, 2011).

To understand the role of autophagy in a developed mammal, we generated a GEMM where we can knock Atg7 throughout the entire mouse by TAM administration. Here we report that, in contrast to neonatal mice that require autophagy for survival, adult mice survive autophagy ablation. Acute, systemic autophagy ablation does, however, shorten lifespan due to neurodegeneration partly due to p53 activation and increased susceptibility to infection. Autophagy is required for adult mice to maintain lipid stores and survive fasting by sustaining glucose homeostasis and suppressing p53. Autophagy deficiency also sensitizes adult mice to γ-irradiation-induced death. This suggests that autophagy is essential for adult mice for long-term survival and to tolerate multiple forms of stress, and the mechanism is completely different from that of neonates.

Results

Acute *Atg7* deletion in adult mice produces systemic autophagy defect

Adult mice were engineered with floxed alleles of *Atg7* (Komatsu et al., 2005) and a transgene expressing the TAM-regulated Cre-recombinase fusion protein under the control of the ubiquitously expressed ubiquitin C (Ubc) promoter (Ruzankina et al., 2007). 8-10 week old adult mice retain intact *Atg7* (wild type mice or mice with *Atg7* floxed alleles with or without the *Ubc-CreERT2* allele) and express ATG7 protein, but when provided TAM, the Cre is activated only in mice with *Atg7* floxed and *Ubc-CreERT2* alleles, deleting the Lox-P sites and *Atg7*, producing a near complete and sustained loss of ATG7 protein ($Atg7^{\Delta/\Delta}$ mice) in all tissues examined by 2 weeks following the last day of 5-day course of TAM administration (Fig. 2.1A-C). *Atg7* deletion throughout mouse tissues was also confirmed by PCR.

The loss of ATG7 correlated with accumulation of the autophagy substrate p62 and the unprocessed form of microtubule-associated protein 1A/1B-light chain 3 (LC3-I) and the absence of the cleaved, lipidated and active (autophagosome associated) form LC3-II (Fig. 2.1B). These findings are consistent with efficient, conditional ablation of ATG7 expression and loss of autophagy in adult mouse tissues, allowing the assessment of the role of autophagy in adult mice for the first time.

Figure 2.1 Conditional whole-body deletion of *Atg7* abrogates autophagy.

A. Experimental design for generation of *Atg7*$^{\Delta/\Delta}$ mice. *Atg7*$^{flox/flox}$ or *Ubc-CreERT2*$^{/+}$;*Atg7*$^{flox/flox}$ mice were treated with TAM at 8-10 week of age by intraperitoneal injection and analyzed at times thereafter.

B. Western blotting for ATG7, p62 and LC3 at the indicated times (w: weeks, m: months) of the indicated tissues from TAM-treated *Atg7*$^{flox/flox}$ or *Atg*$^{\Delta/\Delta}$ adult mice. *Atg7*$^{flox/flox}$ control tissues are from a 5 weeks post-TAM-treated mouse. Tumor derived cell lines (TDCL) from *Atg7*-intact and -deficient tumors (Guo et al., 2013a) were used as controls for ATG7, LC3 and p62 protein expression. β-ACTIN serves a protein loading control.

C. Representative IHC images for ATG7 of indicated tissues from 5 weeks post-TAM-treated *Atg7*$^{flox/flox}$ or *Atg7*$^{\Delta/\Delta}$ adult mice.

D. Representative pictures of 2 months post-TAM-treated *Atg7*$^{flox/flox}$ or *Atg7*$^{\Delta/\Delta}$ female and male mice (n=3 for each genotype).

E. Body weight difference of TAM-treated *Atg7*$^{flox/flox}$ or *Atg7*$^{\Delta/\Delta}$ adult mice at the indicated times (w: weeks, m: months). Error bar represents SEM, *p≤0.05, **p≤0.01 (two-way ANOVA with Bonferroni post-test).

F. Body fat composition as determined by EchoMRI of 10 days post-TAM-treated *Atg7*$^{flox/flox}$ or *Atg7*$^{\Delta/\Delta}$ adult mice. Error bar represents SEM, *p≤0.05 ((two-way ANOVA with Bonferroni post-test).

G. Lean muscle mass as determined by EchoMRI of 10 days post-TAM-treated *Atg7*$^{flox/flox}$ or *Atg7*$^{\Delta/\Delta}$ adult mice. Error bar represents SEM, ***p≤0.001 (two-way ANOVA with Bonferroni post-test).

H. Representative liver weight and liver weight-excluded body weight at indicated times. Error bar represents SEM, *p≤0.05, **p≤0.01 (two-way ANOVA with Bonferroni post-test).

I. Representative spleen weight at indicated times. Error bar represents SEM, **p≤0.01, ***p≤0.001 (two-way ANOVA with Bonferroni post-test).

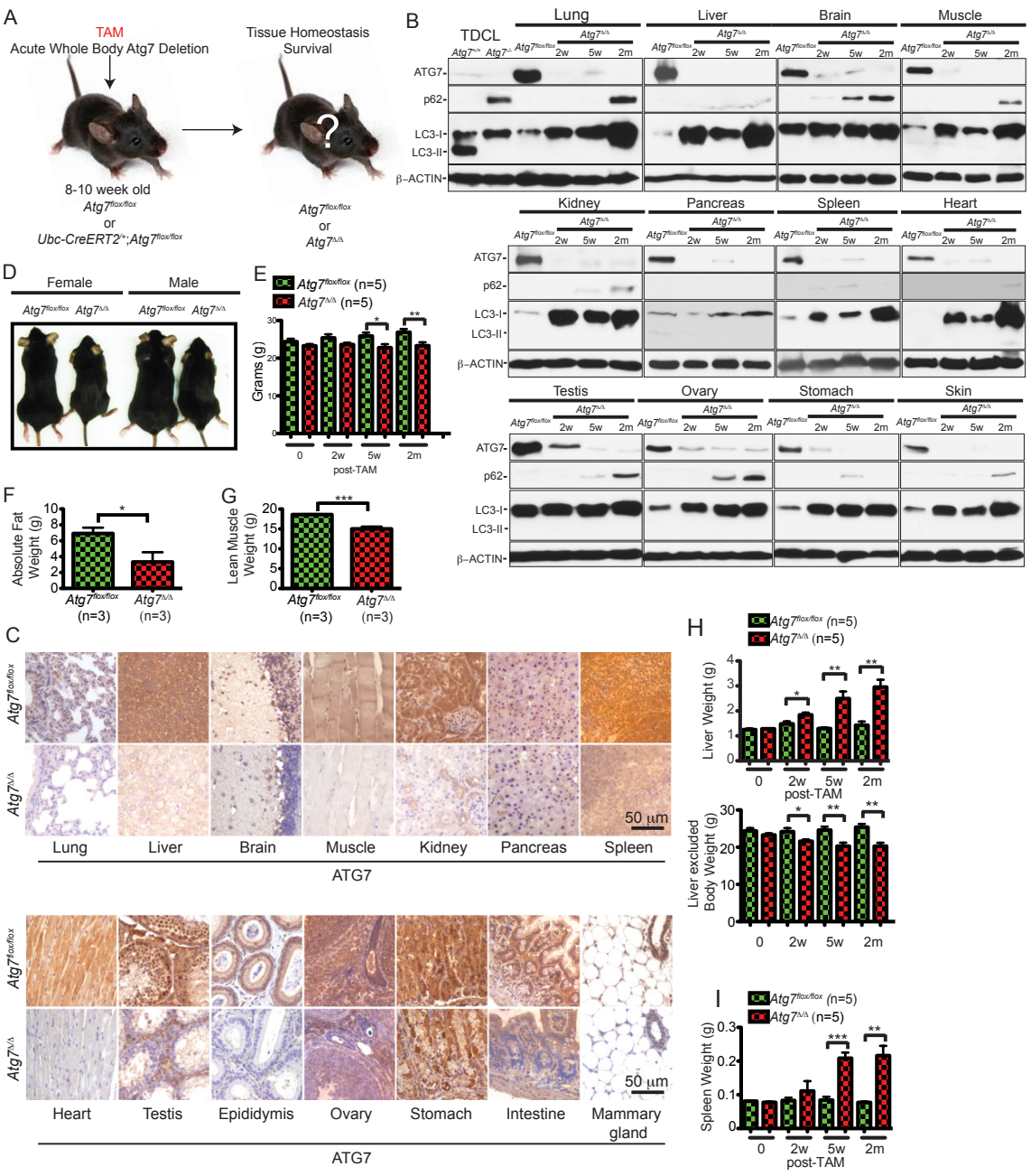

Figure 2.1 Conditional whole-body deletion of *Atg7* abrogates autophagy.

ATG7 deficiency causes depletion of white adipose tissue (WAT) and damage to liver and muscle

In comparison to *Atg7* wild type mice, *Atg7*$^{\Delta/\Delta}$ mice at 2 months post-TAM were smaller in size and had reduced body weight (Fig. 2.1D and E), despite similar feeding behavior and energy expenditure. Liver weight was increased in *Atg7*$^{\Delta/\Delta}$ mice (Fig. 2.1H), consistent with steatosis that results also from liver-specific *Atg7* or *Atg5* deletion (Komatsu et al., 2007; Komatsu et al., 2005; Ni et al., 2012; Takamura et al., 2011). Echo Magnetic Resonance Imaging (EchoMRI) analysis of body composition showed less absolute fat and lean body mass in *Atg7*$^{\Delta/\Delta}$ compared to control mice at 2 months post-TAM (Fig. 2.1F and G) explaining the decreased body size of *Atg7*$^{\Delta/\Delta}$ mice. Histological examination of tissues from the *Atg7*$^{\Delta/\Delta}$ mice revealed limited tissue damage at 5 weeks post-TAM that included the beginning of liver abnormalities, splenic enlargement, testicular degeneration and depletion of the lipid content of WAT (Fig. 2.1I and 2.2A-B). Spleens of *Atg7*$^{\Delta/\Delta}$ mice were enlarged with accumulation of megakaryocytes (Fig. 2.2A) although bone marrow appeared normal. We observed testicular degeneration in *Atg7*$^{\Delta/\Delta}$ mice, which was partially due to Cre toxicity; testes were smaller in *Atg7*$^{\Delta/\Delta}$ mice with elevated p62 aggregates mainly in Leydig cells (Fig. 2.1B and 2.2B).

Autophagy is essential for adipocyte differentiation and formation of WAT (Singh et al., 2009b; Zhang et al., 2009). Here, acute autophagy ablation rapidly depleted lipid stores and reduced established WAT by converting WAT to brown adipose tissue (BAT) or by blocking BAT to WAT transdifferentiation. In contrast,

marked liver, brain, muscle and pancreas damage and further depletion of WAT were apparent in *Atg7*$^{\Delta/\Delta}$ mice at 2 months post-TAM (Fig. 2.2A). Thus, systemic *Atg7* deficiency for 5 weeks produces limited toxicities but this is not the case at 2-3 months.

Tissue damage resulting from acute, systemic *Atg7* deficiency in adult mice for 2 months included increased liver enlargement where hepatocytes accumulated p62 and LC3-I aggregates, mitochondria (as indicated by the mitochondrial marker TOM20) and lipid droplets (Oil red O staining) (Fig. 2.1B and 2.2A and Fig. 2.2C-E). These mice also had decreased number of large pyramidal neurons and Purkinje cells (Fig. 2.2A). At the same time, we observed degenerative changes in muscle with centrally nucleated, small myofibers (Fig. 2.2A). These findings are consistent with a time-dependent destructive effect to normal tissues upon loss of autophagy as reported with tissue-specific knockout of *Atg5* or *Atg7* (Ebato et al., 2008; Hara et al., 2006; Jung et al., 2008; Komatsu et al., 2006; Komatsu et al., 2007; Masiero et al., 2009; Singh et al., 2009b; Zhang et al., 2009).

We also observed intra-acinar vacuolization in the pancreas (Fig. 2.2A). Consistent with the role of autophagy in lipid metabolism, kidney and lung tissues accumulated lipids (Fig. 2.2E). Other tissues were not visibly affected by acute *Atg7* ablation. Interestingly, constitutive autophagy deficiency impairs lung function in neonates (Cheong et al., 2014), but as this did not occur in *Atg7*$^{\Delta/\Delta}$ adult mice, this suggests that developing tissues can be more reliant on autophagy than adult ones.

Figure 2.2 Conditional whole-body deletion of *Atg7* produces systemic autophagy defect.

A. Representative liver, cerebral cortex, cerebellum, muscle, pancreas, spleen and adipose histology (H&E) of TAM-treated *Atg7*$^{flox/flox}$ or *Atg7*$^{\Delta/\Delta}$ adult mice at indicated times. Arrowheads in cerebellum point to purkinje cells, arrowheads in muscle point to centrally nucleated myofibers, arrowheads in pancreas point to intra-acinar vacuolization.

B. Representative testis weight and histology (H&E) of post-TAM-treated *Atg7*$^{flox/flox}$, *Ubc-CreERT2/*$^{+}$ or *Atg7*$^{\Delta/\Delta}$ adult mice at indicated times. IHC staining for p62 shows p62 aggregate accumulation in ATG7-deficient leydig cells at 5 weeks post-TAM.

C. Representative IHC images for p62 of the indicated tissues from 2 months post-TAM-treated *Atg7*$^{flox/flox}$ or *Atg7*$^{\Delta/\Delta}$ adult mice.

D. Representative IHC images for TOM20 of the indicated tissues from 2 months post-TAM-treated *Atg7*$^{flox/flox}$ or *Atg7*$^{\Delta/\Delta}$ adult mice.

E. Representative Oil red O staining of indicated tissues from 2 months post-TAM-treated *Atg7*$^{flox/flox}$ or *Atg7*$^{\Delta/\Delta}$ adult mice.

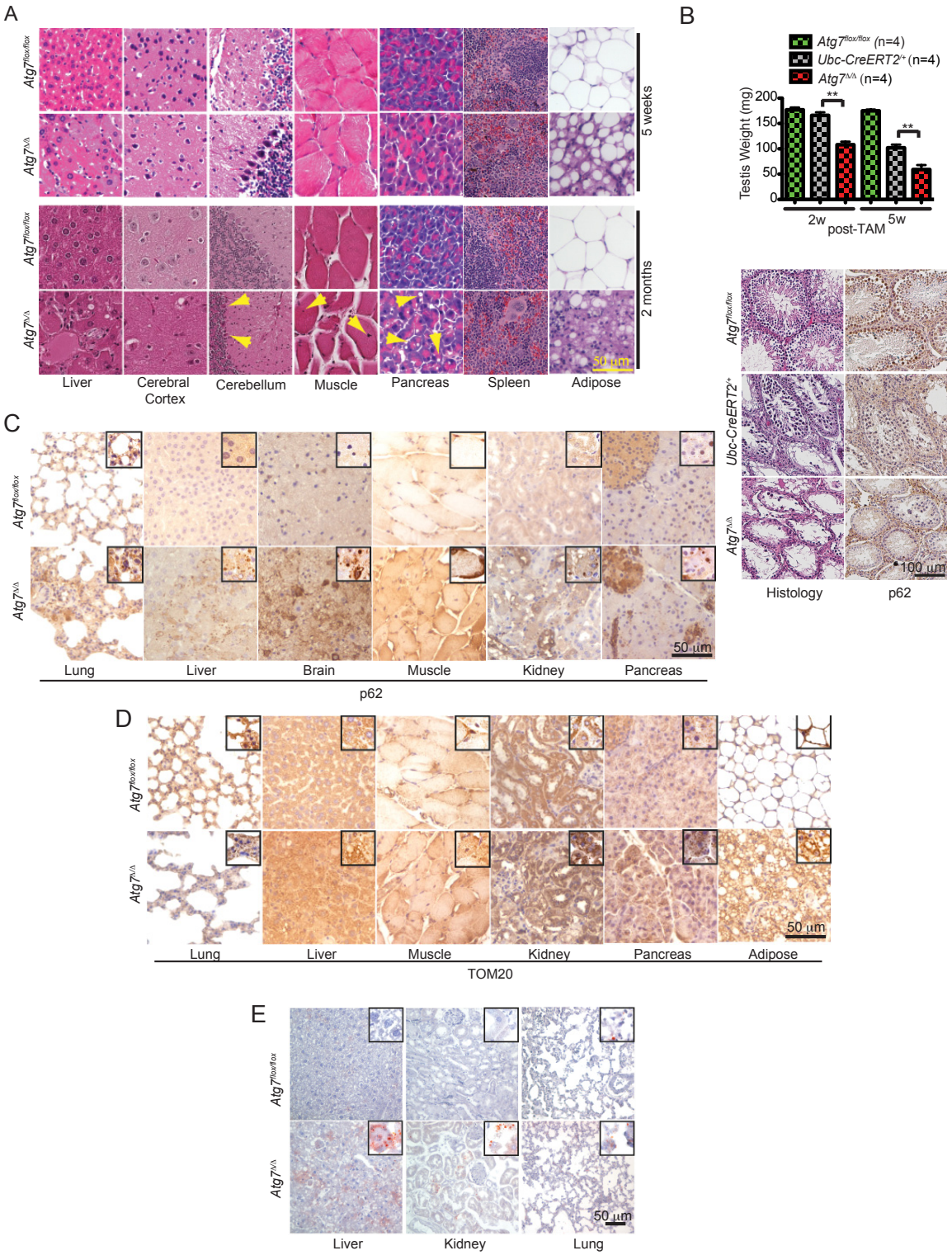

Figure 2.2 Conditional whole-body deletion of *Atg7* produces systemic autophagy defect.

ATG7 extends adult lifespan by suppressing susceptibility to infection and neurodegeneration

A cohort of wild type and *Atg7*$^{\Delta/\Delta}$ mice was followed to assess the consequence to overall survival. Lifespan of *Atg7*$^{\Delta/\Delta}$ mice was shortened to 2-3 months, demonstrating that retention of *Atg7* for functional autophagy is required for the viability of adult mice (Fig. 2.3A). Death of *Atg7*$^{\Delta/\Delta}$ mice resulted from two distinct causes. Several mice (12%) succumbed to *Streptococcus* infection shortly after deletion (Fig. 2.3A, asterisks, and Fig. 2.3B), consistent with the finding that autophagy is required for eliminating intracellular *Streptococcus* in cells *in vitro* (Nakagawa et al., 2004). The vast majority of the *Atg7*$^{\Delta/\Delta}$ mice, however, died between 2-3 months due to neurodegeneration (Fig. 2.3A), similar to findings with neuronal-specific deficiency in *Atg5* or *Atg7* (Hara et al., 2006; Komatsu et al., 2006).

With conditional whole-body deletion of *Atg7* we observed progressive motor and behavioral deficits such as tremors and ataxic walking and limb-clasping reflexes when held by their tails whereas control animals tend to extend their limbs (Supplementary Movie: http://cancerdiscovery.aacrjournals.org/content/suppl/2014/06/10/2159-8290.CD-14-0363.DC1/Vid1.mov). *Atg7*$^{\Delta/\Delta}$ mice also displayed very severely impaired balance and bradykinesia (abnormally slow movements) shortly before death, collectively indicating that death results from neurological defects. Thus the predominant toxicity of autophagy deficiency is neurodegeneration.

Then we turned our attention to identify underlying mechanism of autophagy-induced lethality. Knowing that autophagy deficiency in GEMMs for KRAS- and BRAF-driven lung cancers activates p53 and limits tumor growth (Guo et al., 2013a; Strohecker et al., 2013), we examined the p53 induction in autophagy ablated adult mice. ATG7 deficiency in brain caused p53 induction in neurons (Fig. 2.3C), correlating with more apoptosis when p53 is intact (Fig. 2.3D). We crossed *Ubc-CreERT2/+*;*Atg7* mice to *Trp53*$^{flox/flox}$ mice to generate a conditional model to be *Atg7* deficient together with *p53*, which is activatable by TAM administration. *p53* deletion in autophagy ablated adult mice delayed neurodegeneration dependent death. Despite the reduced apoptosis and prevention of brain damage, the majority of the mice still die later from of ATG7 deficiency (Fig. 2.3E), indicating that the functional status of autophagy dictates the survival and that there are both p53-dependent and –independent mechanisms involved.

Figure 2.3 Conditional whole-body deletion of *Atg7* increases susceptibility to infection and neurodegeneration and impairs long-term survival through p53 activation.

A. Kaplan-Meier survival curve of TAM-treated *Atg7*$^{flox/flox}$ or *Atg7*$^{\Delta/\Delta}$ adult mice (w: weeks, m: months). Asterisks denote mice that died of infection. p≤0.0001 (log-rank Mantel-Cox test).

B. Table for bacterial analysis to identify the cause of septicemia resulting in early lethality of *Atg7*$^{\Delta/\Delta}$ adult mice. Urine and vaginal discharge was collected in sterile conditions and individual colony types were identified using MALDI-TOF spectrometer.

C. Representative IHC images for p53 of the brain sections from 2 weeks post-TAM-treated *Atg7*$^{flox/flox}$ or *Atg7*$^{\Delta/\Delta}$ adult mice.

D. Western blotting for ATG7, p62 and active CASPASE-3 at the indicated times (w: weeks, m: months) of the brain tissues from *Ubc-CreERT2/*$^{+}$, *Atg7*$^{\Delta/\Delta}$, *p53*$^{\Delta/\Delta}$ or *Atg7*$^{\Delta/\Delta}$;*p53*$^{\Delta/\Delta}$ adult mice. β-ACTIN serves a protein loading control.

E. Kaplan-Meier survival curve of *Ubc-CreERT2/*$^{+}$, *Atg7*$^{\Delta/\Delta}$, *p53*$^{\Delta/\Delta}$ or *Atg7*$^{\Delta/\Delta}$;*p53*$^{\Delta/\Delta}$ adult mice. *p≤0.05 (log-rank Mantel-Cox test). Pie charts indicate the relative frequencies of each death cause observed in indicated genotypes for the time period that is circled.

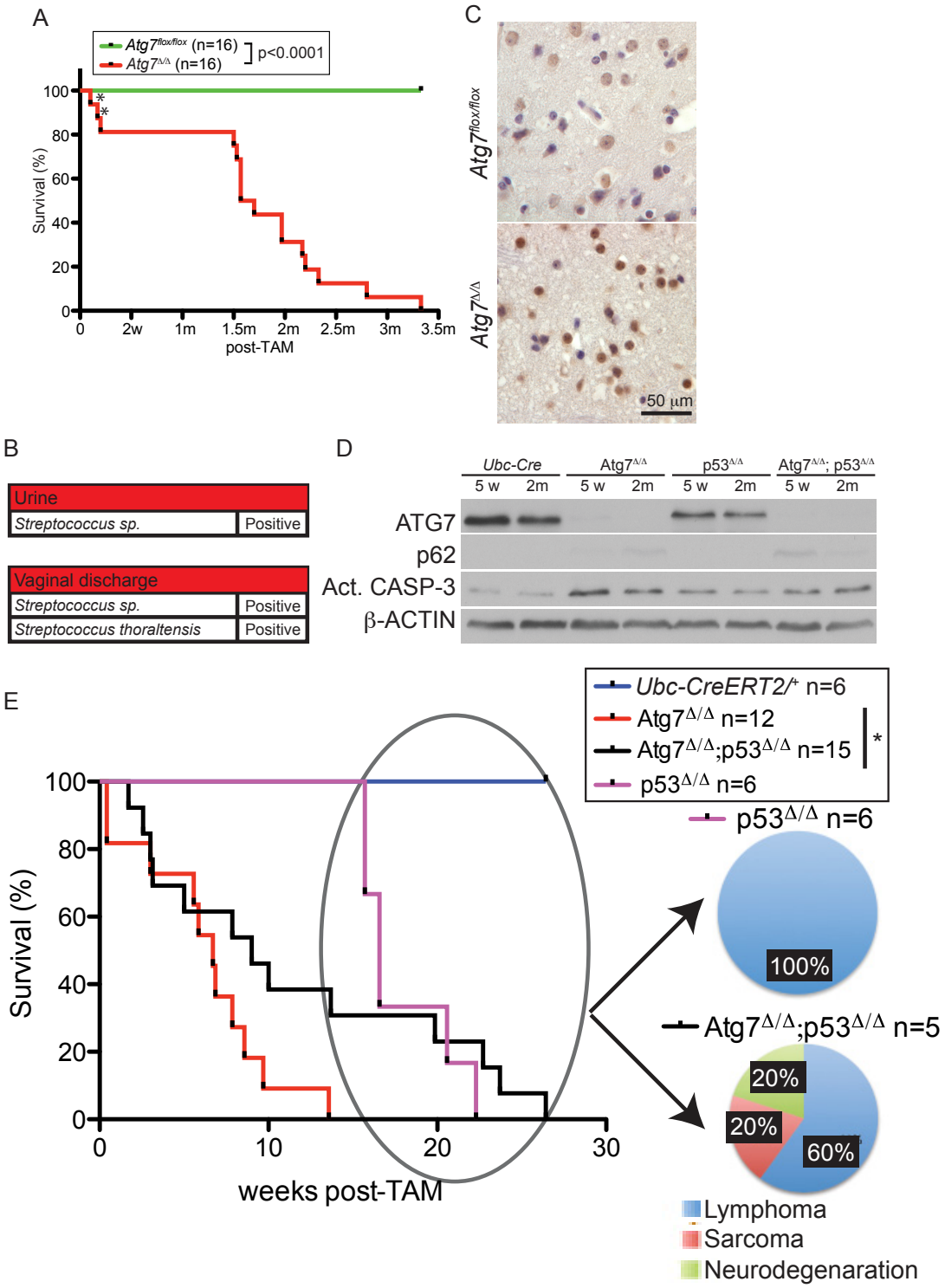

Figure 2.3 Conditional whole-body deletion of *Atg7* increases susceptibility to infection and neurodegeneration and impairs long-term survival through p53 activation.

Autophagy is required for adult mice to survive fasting

The above analysis focused on unstressed mice. A major function of autophagy conserved from yeast to mammals is stress survival. This is evident in the requirement of autophagy to survive the stress of the neonatal starvation period (Komatsu et al., 2005; Kuma et al., 2004). Similarly, autophagy is robustly induced in adult mouse tissues in response to starvation (Mizushima et al., 2004). To test if autophagy is functionally important for adult mice to survive fasting, *Atg7* was deleted in 8-10 week old mice by TAM administration (mice with *Atg7* floxed alleles plus the *Ubc-CreERT2* allele; $Atg7^{\Delta/\Delta}$) or left intact (mice with *Atg7* floxed alleles without the *Ubc-CreERT2* allele; $Atg7^{flox/flox}$).

10 days following the last day of a 5-day schedule of TAM administration when ATG7 expression was extinguished (Fig. 2.4A), mice were subjected to fasting (free access to water without food) for 24 hours. We chose this short-term autophagy inactivation to establish the acute and direct requirement for autophagy. All fed mice (*Atg7* intact or $Atg7^{\Delta/\Delta}$) and all fasted mice with *Atg7* intact survived for 24 hours as expected (Fig. 2.4B). In contrast, the majority of $Atg7^{\Delta/\Delta}$ mice failed to survive fasting for 24 hours (Fig. 2.4B). Thus, similar to neonates, adult mice also require autophagy to tolerate starvation. Serum insulin and leptin levels were downregulated by fasting independent of autophagy status (Fig. 2.4C), suggesting that the hormonal response to starvation was normal and thus not the cause of the fasting lethality of ATG7-deficient mice.

Figure 2.4 Autophagy is required for adult mice to survive fasting.

A. ATG7 Western blot of tissue lysates from *Atg7*$^{flox/flox}$ or *Atg7*$^{\Delta/\Delta}$ adult mice 10 days post-TAM-treated, fed and fasted. β-ACTIN serves a protein loading control.

B. Kaplan-Meier survival curve of *Atg7*$^{flox/flox}$ or *Atg7*$^{\Delta/\Delta}$ adult mice 10 days post-TAM-treated fed and fasted; p=0.0072 (log-rank Mantel-Cox test).

C. Quantification of serum insulin (left) and leptin (right) levels of 10 days post-TAM-treated fed or fasted, *Atg7*$^{flox/flox}$ or *Atg7*$^{\Delta/\Delta}$ adult mice. Error bar represents SEM, *p≤0.05 (two-way ANOVA with Bonferroni post-test).

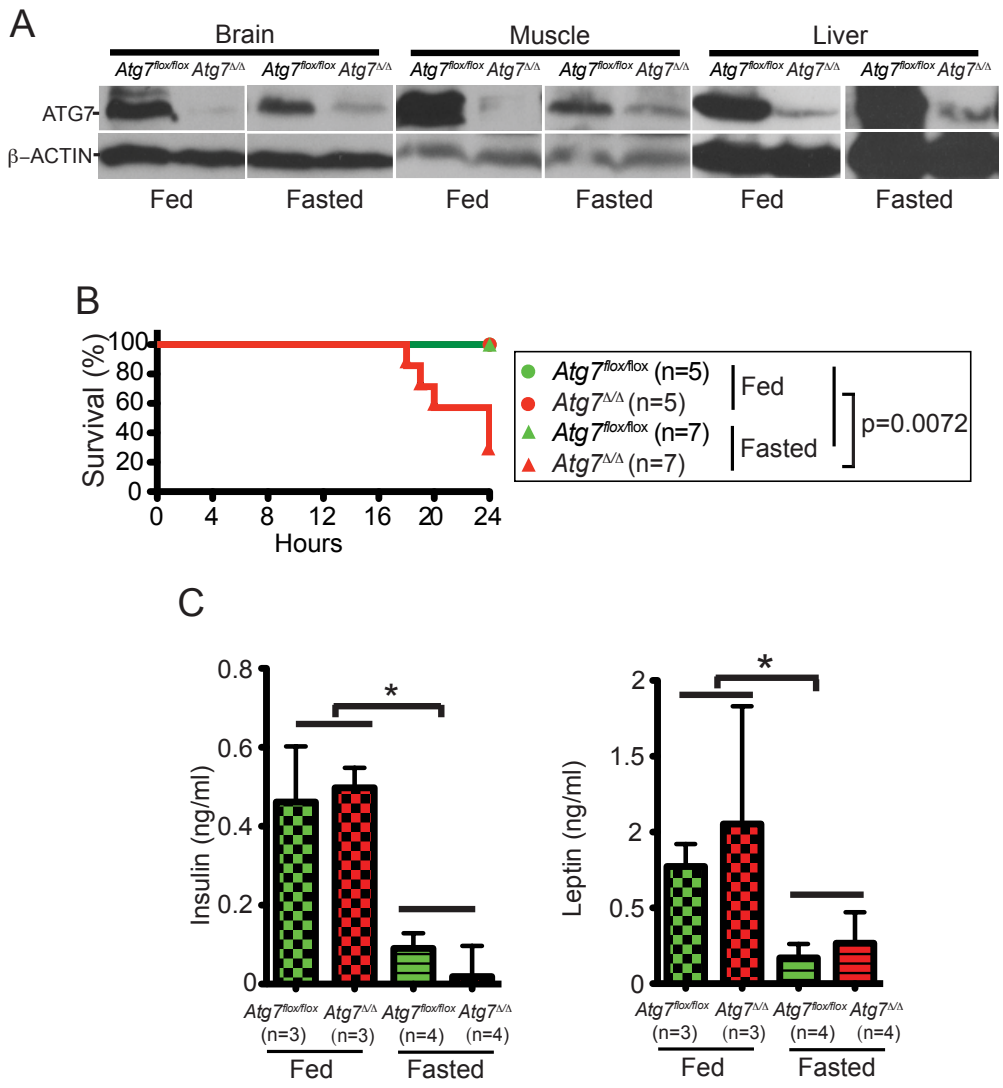

Figure 2.4 Autophagy is required for adult mice to survive fasting.

Autophagy maintains fat stores and the mobilization of lipids during fasting

The physiology and metabolic requirements of neonates are distinct from that of adult mice, raising the question as to whether the role of autophagy in supporting survival during fasting also differed. Neonates require autophagy to maintain serum amino acid but not glucose levels (Kuma et al., 2004). To address the mechanism by which autophagy contributes to the survival of adult mice during fasting, tissues and serum were examined during fed and fasted conditions in the presence and absence of ATG7.

There was a striking depletion of WAT, apparent with short-term *Atg7* deletion under fed conditions (Fig. 2.5A). Histological examination revealed marked reduction of epididymal adipose mass due to a reduction in the size of fat droplets in $Atg7^{\Delta/\Delta}$ mice in the short term and accumulation of mitochondria (Fig. 2.5A and 2.2D). Thus, the presence of ATG7 favors WAT whereas ATG7 deficiency favors BAT. To assess absolute total body fat mass, live *Atg7* intact or $Atg7^{\Delta/\Delta}$ mice were subjected to EchoMRI. Fed $Atg7^{\Delta/\Delta}$ mice displayed reduced absolute fat mass compared to mice with *Atg7* intact, indicating that acute autophagy deficiency causes depletion of fat stores (Fig. 2.5B). ATG7 promotes adipose differentiation favoring BAT formation, possibly due to a decreased capacity for lipid storage and increased lipid metabolism through β-oxidation. This suggests that the reduction in dedicated lipid stores may compromise survival during fasting. Indeed, fat mass was more severely depleted in fasted $Atg7^{\Delta/\Delta}$ mice than in those with *Atg7* intact (Fig. 2.5B). Mobilization of FFAs in

serum during fasting was also defective without ATG7, revealing a metabolic deficiency that can contribute to lethality (Fig. 2.5C).

Glycogen stores are depleted in fasted ATG7-deficent mice

Glycogen store mobilization, particularly in liver, provides an important source of glucose in fasted conditions that contributes to serum glucose homeostasis. Fasting reduced liver size to a greater extent in *Atg7*$^{\Delta/\Delta}$ mice (17% with *Atg7* intact, compared to a 29% in *Atg7*$^{\Delta/\Delta}$ mice), and these mice had higher serum levels of the liver enzymes aspartate aminotransferase (AST) and alanine aminotransferase (ALT) when fasted, indicative of some liver damage. Indeed, these mice had increased apoptosis coincident with DNA damage response activation (γ-H2AX positive hepatocytes) although healthy liver tissue was still present (Fig. 2.5D and E). Importantly, in contrast to fasted *Atg7*-intact mice, fasted *Atg7*$^{\Delta/\Delta}$ mice had complete depletion of liver glycogen stores (Fig. 2.5E). Thus, autophagy is critical to prevent depletion of glycogen stores during fasting. Since acute deficiency in *Atg7* produced accelerated depletion of lipid and glycogen stores, this indicates a systemic requirement for autophagy that may contribute to their failure to tolerate fasting.

ATG7 prevents muscle wasting during fasting

Degradation of muscle protein sustains homeostasis during fasting (Schiaffino et al., 2013). Gastrocnemius muscle mass was slightly reduced in *Atg7*$^{\Delta/\Delta}$ mice with short-term deletion under fed condition in comparison to that from *Atg7* intact mice (Fig. 2.5F), as was a reduction in total muscle mass revealed by EchoMRI (Fig. 2.5G). Fasting, however, induced severe muscle wasting with

DNA damage response activation (γ-H2AX positive myofibers) in *Atg7*$^{\Delta/\Delta}$ compared to *Atg7*-intact mice (Fig. 2.5F). Thus, without autophagy, fasting induces severe muscle wasting. Ultimately, metabolic failure can lead to brain damage and death. In contrast to fed and fasted mice with *Atg7* intact, fasted *Atg7*$^{\Delta/\Delta}$ mice showed loss of motor control indicative of neurologic impairment, which was consistent with the occurrence of extensive brain damage (Fig. 2.5H).

Figure 2.5 Autophagy is required for adult mice to survive fasting.

A. Representative male pictures (left), tissue weight (middle) and histology (H&E) (right) of epididymal adipose tissues of *Atg7*$^{flox/flox}$ or *Atg7*$^{\Delta/\Delta}$ adult mice 10 days post-TAM-treated fed and fasted (n=4, for each). Error bar represents SEM, *p≤0.05 (two-way ANOVA with Bonferroni post-test).

B. Body fat composition as determined by EchoMRI of *Atg7*$^{flox/flox}$ or *Atg7*$^{\Delta/\Delta}$ adult mice 10 days post-TAM-treated. Error bar represents SEM, *p≤0.05 (two-way ANOVA with Bonferroni post-test).

C. Quantification of serum FFA levels of *Atg7*$^{flox/flox}$ or *Atg7*$^{\Delta/\Delta}$ adult mice 10 days post-TAM-treated fed and fasted. Error bar represents SEM, *p≤0.05 (two-way ANOVA with Bonferroni post-test).

D. Liver weight (left) and serum level of liver enzymes AST (middle) and ALT (right) from *Atg7*$^{flox/flox}$ or *Atg7*$^{\Delta/\Delta}$ adult mice 10 days post-TAM-treated fed and fasted. Error bar represents SEM, **p≤0.01 (two-way ANOVA with Bonferroni post-test).

E. Representative liver histology (H&E) and liver glycogen levels (PAS staining) of *Atg7*$^{flox/flox}$ or *Atg7*$^{\Delta/\Delta}$ adult mice 10 days post-TAM-treated fed and fasted. Arrowheads point to glycogen. IHC staining for Active Caspase-3 shows apoptosis induction and IHC staining for γ-H2AX shows DNA damage response activation in ATG7-deficient liver tissue when fasted.

F. Representative gross image of calf muscle (left) and weight of gastrocnemius muscle and representative muscle histology (H&E) from

Atg7$^{flox/flox}$ or *Atg7*$^{\Delta/\Delta}$ adult mice 10 days post-TAM-treated fed and fasted. IHC staining for γ-H2AX shows DNA damage response activation in ATG7-deficient muscle tissue when fasted. Error bar represents SEM, **p≤0.01 (two-way ANOVA with Bonferroni post-test).

G. Lean muscle mass as determined by EchoMRI of *Atg7*$^{flox/flox}$ or *Atg7*$^{\Delta/\Delta}$ adult mice 10 days post-TAM-treated. Error bar represents SEM, ***p≤0.001 (two-way ANOVA with Bonferroni post-test).

H. Representative brain histology (H&E) of *Atg7*$^{flox/flox}$ or *Atg7*$^{\Delta/\Delta}$ adult mice 10 days post-TAM-treated fed and fasted. IHC staining for γ-H2AX shows DNA damage response activation in ATG7-deficient brain tissue when fasted.

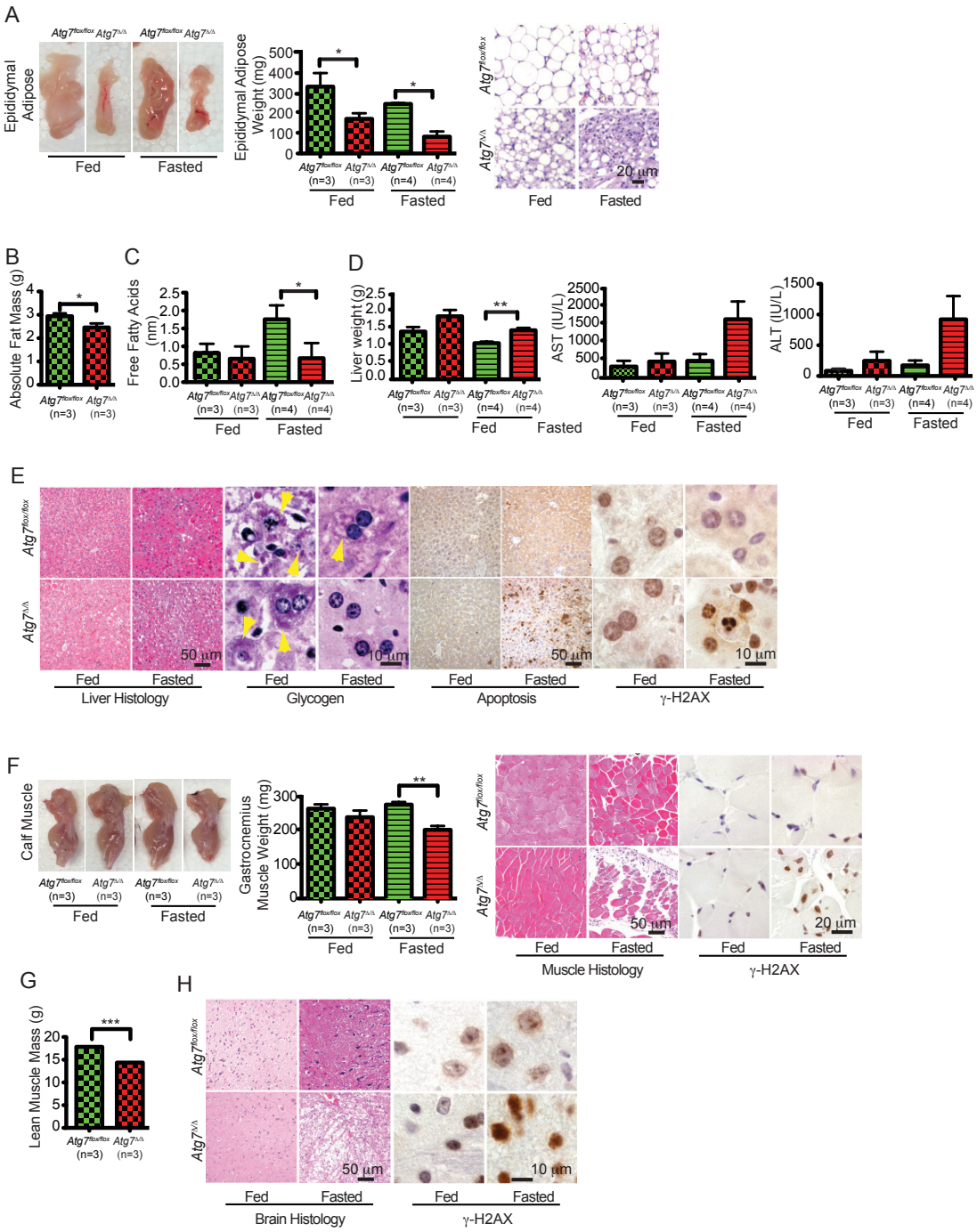

Figure 2.5 Autophagy is required for adult mice to survive fasting.

Fasted *Atg7*-deficient adult mice die from hypoglycemia

To address the mechanism by which autophagy sustains mouse survival during fasting, we first examined levels of serum amino acids by Liquid Chromatography-Mass Spectrometry (LC-MS) in fed and fasting conditions, in *Atg7* intact and $Atg7^{\Delta/\Delta}$ mice. In contrast to *Atg7*-deficient neonates undergoing neonatal starvation, adult $Atg7^{\Delta/\Delta}$ mice with short-term *Atg7* deletion sustained serum amino acid levels with the exception of arginine (Fig. 2.6A). Serum β-hydroxybutyrate levels were elevated in fasting in both *Atg7* intact and $Atg7^{\Delta/\Delta}$ mice, suggesting that serum amino acids were sufficient to induce ketogenesis (Fig. 2.6B). Extensive muscle wasting in fasted $Atg7^{\Delta/\Delta}$ mice may sustain serum amino acids and ketogenesis, partly compensating for depleted fat and glycogen stores.

We next examined serum glucose levels and found that the majority of fasted $Atg7^{\Delta/\Delta}$ mice were severely hypoglycemic consistent with loss of viability (Fig. 2.6C). Indeed, glucose supplementation was sufficient to rescue serum glucose levels, muscle wasting and survival of fasted $Atg7^{\Delta/\Delta}$ mice (Fig. 2.6D). Thus, autophagy in adult mice is required to maintain fasting serum glucose levels, preventing hypoglycemia and death, revealing different metabolic roles for autophagy in the systemic metabolism of neonatal and adult mice.

Atg7 deletion alters gene expression responses to fasting

Functional analysis of differentially expressed genes revealed that molecular functions related to inflammatory response were highly enriched in livers from $Atg7^{\Delta/\Delta}$ mice (Fig. 2.6E and 2.7A). This suggests that liver function is altered by

Atg7 deficiency under fed conditions, although this was not the case for muscle, consistent with normal histology (Fig. 2.2A). Fasting *Atg7*-intact mice repressed gene expression for lipid metabolic processes and insulin signaling and elevated those for fatty acid oxidation in liver (Fig. 2.6F) but induced few changes in muscle gene expression (Fig. 2.6F, and 2.7B). Fasting $Atg7^{\Delta/\Delta}$ mice reduced signatures for liver immune response-related genes; however, there was not a significant change in lipid metabolism-related gene expression as opposed to *Atg7*-intact mice (Fig. 2.6G and 2.7A).

Gluconeogenesis predominantly occurs in the liver, producing glucose that supports metabolism in the brain and other tissues. Genes associated with gluconeogenesis were induced by fasting in liver in $Atg7^{\Delta/\Delta}$ mice (e.g. *Ppargc1a, Atf4, Arntl, Pdk4, Got1, Lepr*) (Fig. 2.7A and C) suggesting that it may be defective because of insufficient substrates. For example, depletion of FFAs may cause more use of amino acids for ketogenesis instead of gluconeogenesis. Depletion of WAT would limit the availability of glycerol for use as a substrate for gluconeogenesis. Fasting caused activation of catabolic processes for autophagy and atrophy (e.g. *Ulk1*, *Bnip3*, *Foxo1*, *Fbxo32*, *Mt1* and *Mt2*) (Fig. 2.6G, 2.7B and D-E). The muscle atrophy signature in the fasted $Atg7^{\Delta/\Delta}$ mice is consistent with extensive muscle wasting.

In summary, healthy adult mice have lipid and glycogen stores that are mobilized during fasting, reducing the demand for muscle catabolism to supply amino acids for gluconeogenesis. Liver and muscle autophagy may also supply substrates for gluconeogenesis. Lipid and glycogen stores in $Atg7^{\Delta/\Delta}$ mice were

depleted even under fed conditions, and fasting accelerates glycogen elimination and caused excessive muscle wasting (Fig. 2.8). While serum amino acid levels and ketogenesis were sustained in *Atg7*$^{\Delta/\Delta}$ mice, they died nonetheless from hypoglycemia. Therefore, this suggests that adult mice require autophagy to provide substrates for glucose homeostasis to survive fasting.

Figure 2.6 Autophagy sustains glucose homeostasis required to survive fasting.

A. Quantification of serum amino acid levels in *Atg7*$^{flox/flox}$ or *Atg7*$^{\Delta/\Delta}$ adult mice 10 days post-TAM-treated fed and fasted. BCAA: branched chain amino acid. Error bar represents SEM, *p≤0.05, **p≤0.01 (two-way ANOVA with Bonferroni post-test).

B. Quantification of serum β-hydroxybutyrate levels in *Atg7*$^{flox/flox}$ or *Atg7*$^{\Delta/\Delta}$ adult mice 10 days post-TAM-treated fed and fasted. Error bar represents SEM, *p≤0.05 (two-way ANOVA with Bonferroni post-test).

C. Quantification of blood glucose levels of *Atg7*$^{flox/flox}$ or *Atg7*$^{\Delta/\Delta}$ adult mice 10 days post-TAM-treated fed and fasted. Error bar represents SEM, *p≤0.05 (two-way ANOVA with Bonferroni post-test).

D. Kaplan-Meier survival curve (left), serum glucose levels (middle) and weight of gastrocnemius muscle (right) from *Atg7*$^{\Delta/\Delta}$ adult mice 10 days post-TAM-treated, fasted, without or with glucose supplemented p=0.0022 (log-rank Mantel-Cox test). Error bar represents SEM, *p≤0.05, **p≤0.01 (two-way ANOVA with Bonferroni post-test).

E-G. Analysis of differentially expressed genes from liver and muscle tissue in *Atg7*$^{flox/flox}$ or *Atg7*$^{\Delta/\Delta}$ adult mice 10 days post-TAM-treated, fed and fasted showing upregulated (blue) or downregulated (pink) genes for significant biological processes as determined by GO term DAVID Analysis. Number scale represents the number of up- (positive number) and down- (negative number) regulated genes in the indicated biological processes.

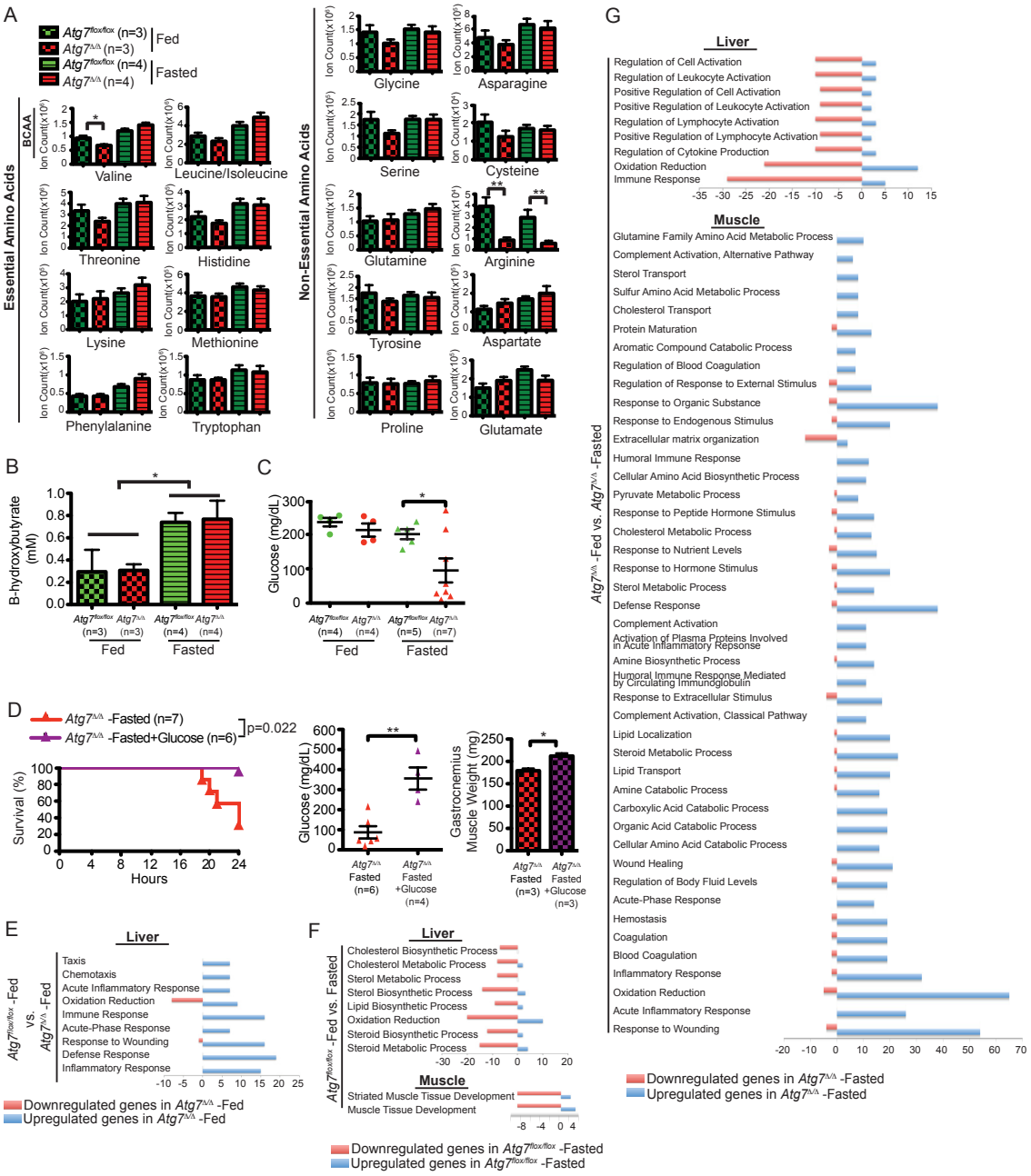

Figure 2.6 Autophagy sustains glucose homeostasis required to survive fasting.

Figure 2.7 Heatmaps for differentially expressed genes.

A. Heatmap for union of differentially expressed genes (fold change>3) in liver comparing *Atg7*$^{flox/flox}$ fed to fasted and to *Atg7*$^{\Delta/\Delta}$ fed and fasted 10 days post-TAM. Scale bar represents $\log_2$ transformed signal intensities.
B. Heatmap for union of differentially expressed genes (fold change>3) in muscle comparing *Atg7*$^{flox/flox}$ fed to fasted and to *Atg7*$^{\Delta/\Delta}$ fed and fasted 10 days post-TAM. Scale bar represents $\log_2$ transformed signal intensities.
C. Selected gluconeogenesis-related genes from A.
D. Selected atrophy-related genes from B.
E. Selected autophagy-related genes from B.

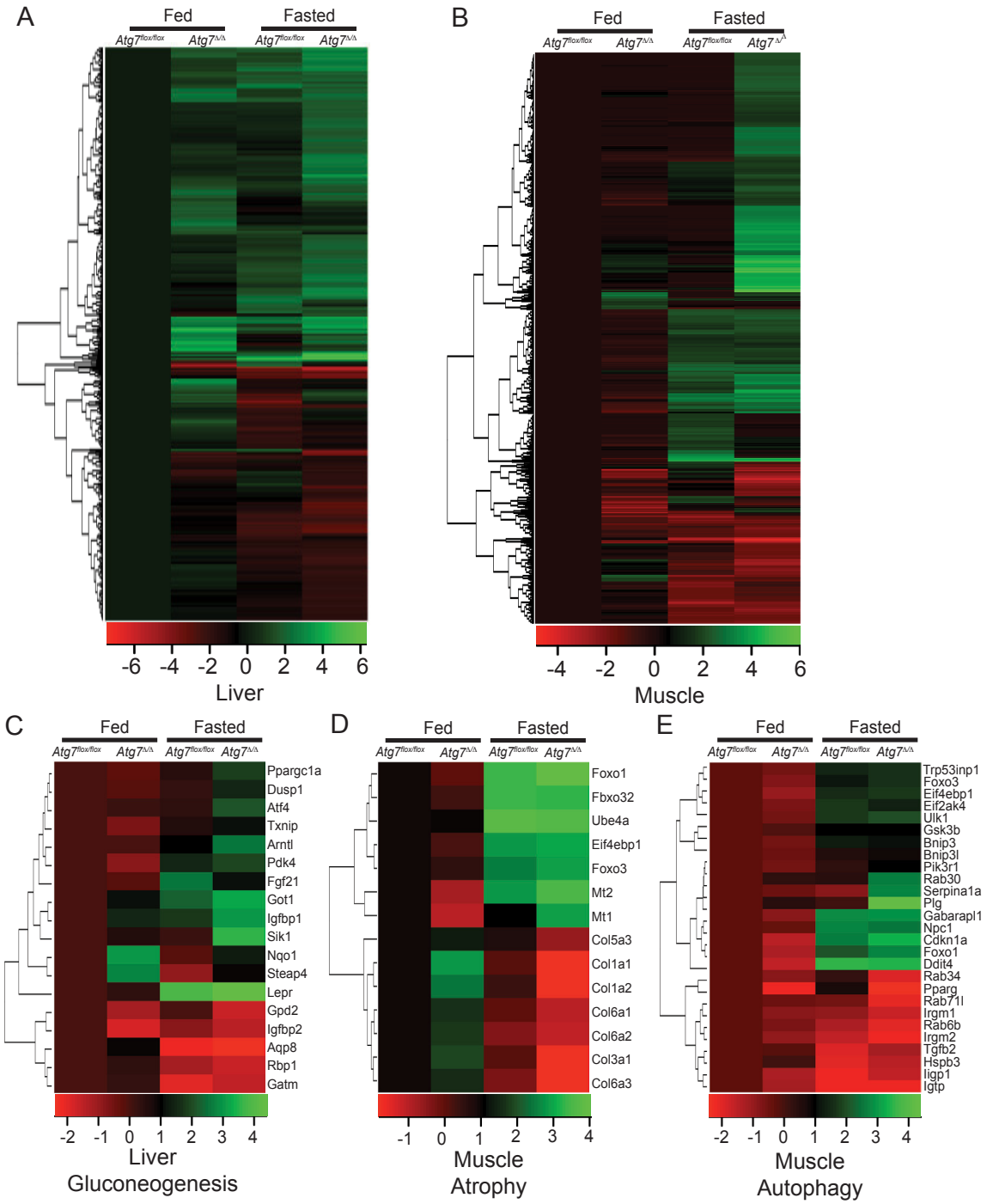

Figure 2.7 Heatmaps for differentially expressed genes.

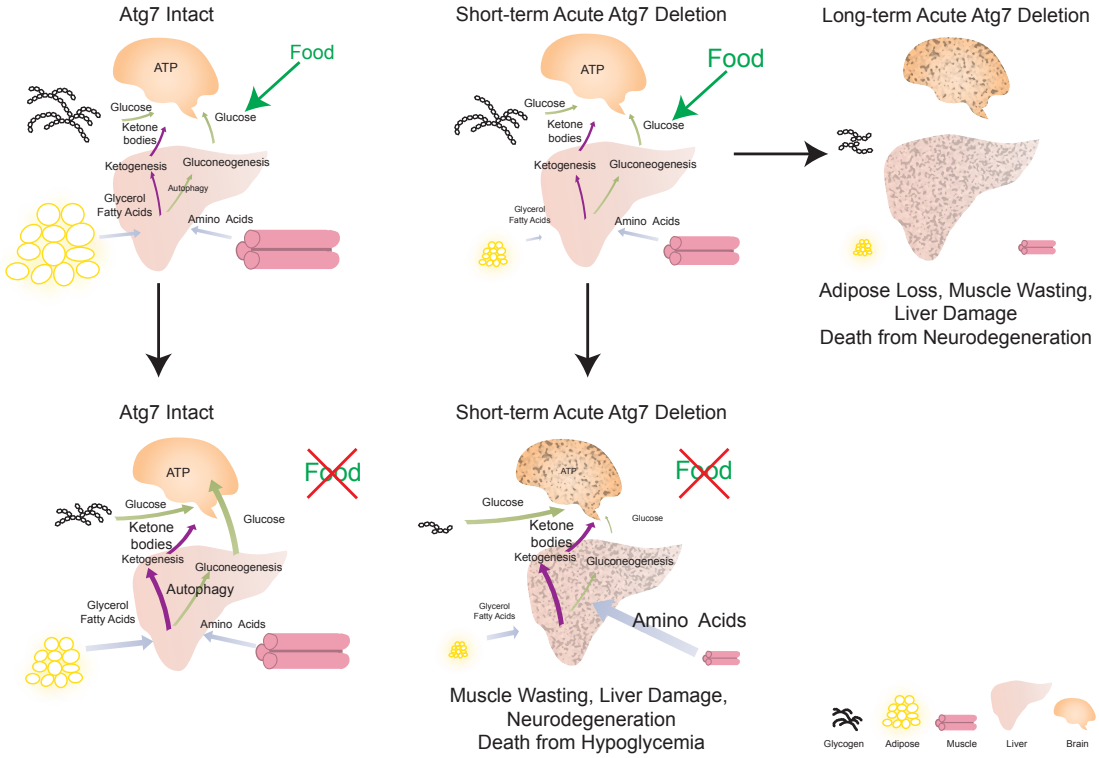

Figure 2.8 Mechanism by which autophagy supports survival of adult mice during fasting. See text for details.

When mice are fasted, they die of neurodegeneration due to hypoglycemia. Similar to what was observed in long-term autophagy ablation-induced neurodegeneration, p53 was also induced in autophagy deficient mouse brain following fasting (Fig. 2.9A). Although the mice were suffering from hypoglycemia, this was not detrimental to *Atg7* deleted mice when p53 is ablated (Fig. 2.9B-C). This finding suggests that p53 mediates lethality in response to starvation of ATG7 deficient mice (Fig. 2.9D).

Figure 2.9 ATG7 regulates p53-dependent survival.

A. Representative IHC images for p53 of brain tissues of *Ubc-CreERT2*$^{+/-}$ or *Atg7*$^{\Delta/\Delta}$ adult mice 10 days post-TAM-treated and fasted.

B. Kaplan-Meier survival curve of fasted adult mice at 10 days post-treatment. *p≤0.05 (log-rank Mantel-Cox test).

C. Quantification of blood glucose levels of fasted adult mice at 10 days post-treatment. Error bar represents SEM, *p≤0.05, **p≤0.01 (two-way ANOVA with Bonferroni post-test).

D. A model showing how ATG7 regulates p53-dependent survival.

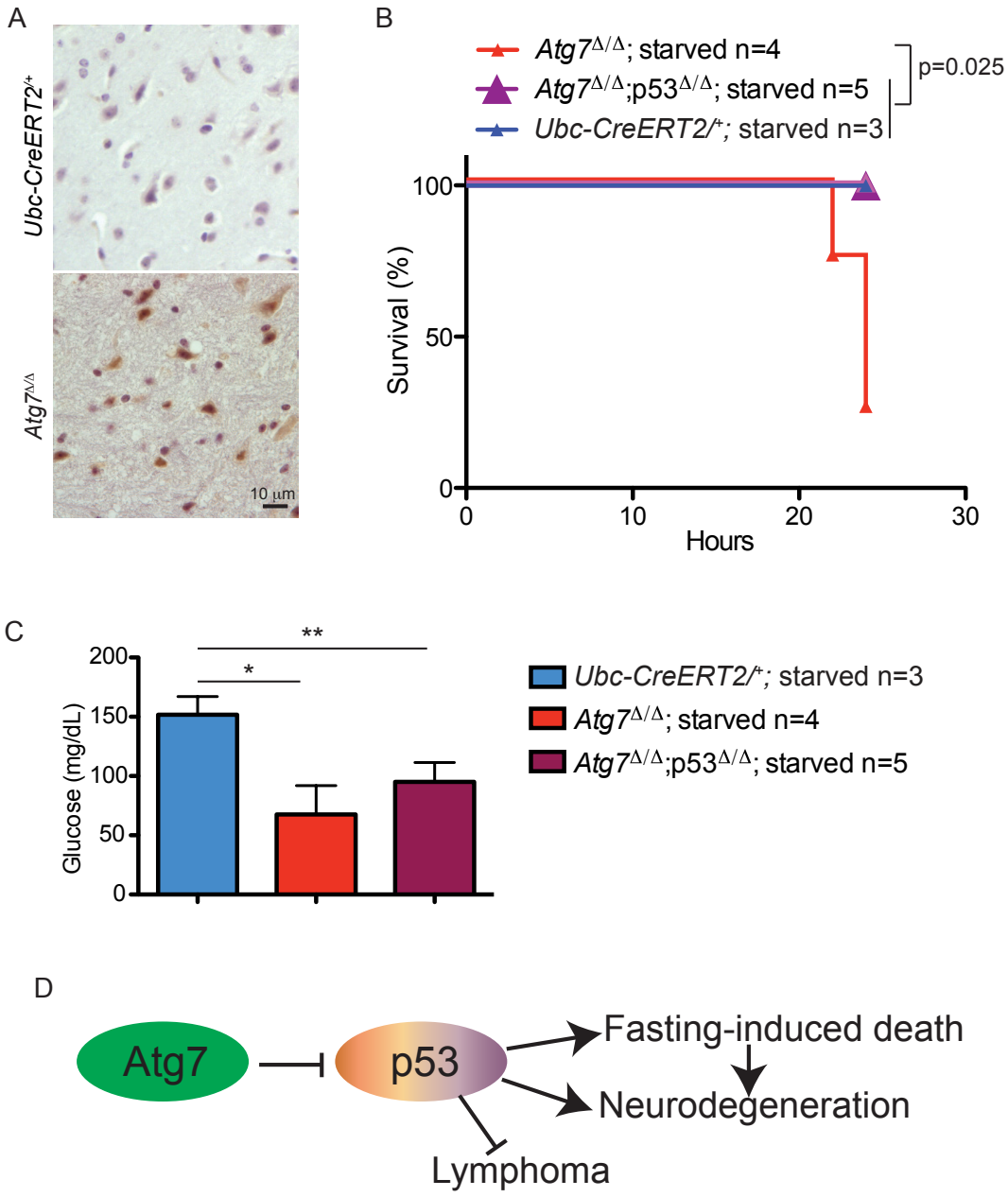

Figure 2.9 ATG7 regulates p53-dependent survival

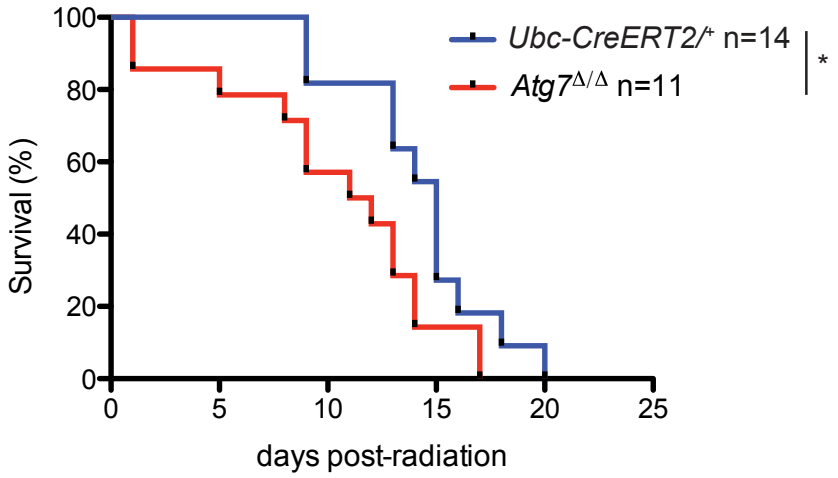

Figure 2.10 *Atg7* deficiency sensitizes to γ-irradiation induced death. Kaplan-Meier survival curve of *Ubc-CreERT2*$^{/+}$ or *Atg7*$^{\Delta/\Delta}$ adult mice following exposure to 10 Gy of whole-body ionizing radiation. *p≤0.05 (log-rank Mantel-Cox test).

Discussion

Acute autophagy ablation using conditional whole-body deletion of *Atg7* in adult mice demonstrated the essential, systemic role of autophagy in host defense against *Streptococcus* infection and in preventing neurodegeneration that together limit lifespan to no more than 3 months (Karsli-Uzunbas et al., 2014). This contrasts constitutive autophagy-deficient mice where neonates fail to survive much more than 24 hours after birth even when force-fed (Komatsu et al., 2005; Kuma et al., 2004), suggesting that autophagy is more critical in newborn than adult mice.

The autophagy deficient mice activate p53 in brain tissue similar to that observed in autophagy-ablated tumor tissues (Guo et al., 2013a; Strohecker et al., 2013). When we co-delete *p53* and *Atg7* in adult mice; neurodegeneration is not totally rescued but delayed for an average of 3 weeks. In parallel with delayed brain damage, apoptotic response induced by autophagy deletion was also suspended with p53 ablation. This data suggest a model where autophagy protects adult mammals from neurodegeneration in a p53 dependent manner in the short-term. In the long term, other pathways promote death of mice with ATG7 deficiency.

Loss of autophagy in adult mice rapidly decreases the mass of WAT suggesting that autophagy deficiency creates systemic metabolic deficiency even under fed conditions (Karsli-Uzunbas et al., 2014). Autophagy deficiency may necessitate the catabolism of dedicated fat stores in WAT by cytosolic lipases or may cause browning of adipose tissue that increases β-oxidation and lipid

consumption, which is consistent with mitochondrial accumulation (Singh and Cuervo, 2012). This defective adipose homeostasis and mobilization of FFAs in starved ATG7-deficient mice can contribute to systemic metabolic impairment.

One property common to adult and neonatal mice is the requirement for autophagy to survive starvation, although the underlying mechanisms appear distinct. In contrast to wild type adult mice, we found that those with acute autophagy ablation are intolerant to fasting and die of hypoglycemia (Karsli-Uzunbas et al., 2014). As WAT is depleted in autophagy-deficient mice, fasting results in accelerated depletion of glycogen stores and excessive muscle catabolism in comparison to wild type mice. The autophagy-deficient adult mice sustain serum amino acid levels and ketogenesis, but not FFA and glucose levels, indicating that gluconeogenesis in the liver is insufficient for survival (Karsli-Uzunbas et al., 2014). Moreover, despite excessive muscle wasting and maintenance of serum amino acid levels, this is apparently insufficient for gluconeogenesis. This suggests that liver autophagy and catabolism of lipid stores may be critical either directly or indirectly for gluconeogenesis and glucose homeostasis during fasting.

The fasted autophagy-deficient mice display rapid liver, muscle and brain damage demonstrating the essential requirement for systemic autophagy to survive fasting. Thus, autophagy is required by both neonates and adults to survive starvation but for different reasons. Neonates need autophagy to generate amino acids to sustain metabolic homeostasis, in contrast to adult mice that need autophagy to prevent fatal hypoglycemia. Fasted adult mice deficient

for autophagy have depleted lipid stores and compensate for metabolic impairment by extensive muscle wasting, which is ultimately insufficient for viability (Karsli-Uzunbas et al., 2014). Liver-specific deficiency in autophagy is not fatal to fasted mice (Ezaki et al., 2011; Komatsu et al., 2005), suggesting that autophagy in other tissues, most likely including WAT (which is lost in the absence of autophagy), is essential for survival and glucose homeostasis.

p53 deletion does not rescue hypoglycemia that is caused by autophagy deficiency, but rescues hypoglycemia-induced death. Thus, the impaired glucose homeostasis is associated only with autophagy deficiency. However, there is a correlation between autophagy deficiency and p53 induction in response to neurodegeneration, illustrating a possible role for ATG7 regulating p53 induction. The mechanism underlying this collaboration is not clear, one possibility is p53 deletion might alter lipid metabolism. To further support this idea, FFA levels and collaboration with other signaling pathways should be explored.

In order to understand the role of autophagy in other stress responses, we irradiated mice at a lethal dose. Surprisingly, autophagy deficiency sensitizes mice to γ-irradiation induced death, demonstrating a new role for autophagy in adult mammals. Despite of the tolerance to short term autophagy ablation, these findings point out the essential role of autophagy for stress survival for the first time.

CHAPTER 4

AUTOPHAGY IS REQUIRED FOR LUNG TUMOR MAINTANENCE

Summary

Cancer cells with activating mutations in *Ras* require autophagy to tolerate metabolic stress and for tumorigenesis. Autophagy inhibition may be a potential approach in cancer therapy. However, whether or not autophagy inhibition would selectively compromise tumorigenesis while sparing normal tissues is unknown. For this purpose, we made a mouse model to generate tumors in the lung by activating RAS and deleting *p53*, and then acutely and systemically ablate autophagy by deleting *Atg7* ubiquitously in both normal and tumor tissues. Our previous study revealed that autophagy ablation in the short term is tolerable in adult mice, which provides us a potential therapeutic window. 5 weeks of acute, systemic autophagy ablation was selectively destructive to established tumors compared to normal tissues. Moreover, the anti-tumor activity of ATG7 ablation was greater with systemic compared to tumor-specific deletion suggesting that autophagy in normal tissues promotes tumorigenesis. Indeed, host autophagy, in addition to tumor-intrinsic autophagy, contributed to tumorigenesis. These results provide the preclinical evidence that strategies to inhibit autophagy may be therapeutically advantageous for Ras-driven cancers.

Introduction

Autophagy has a context-dependent role in cancer (White, 2012). It is upregulated and required for the survival of tumor cells in hypoxic tumor regions (White, 2012). Oncogenic Ras transformation upregulates basal autophagy required for maintenance of mitochondrial metabolism and progression of tumorigenesis (Guo et al., 2011; Lock et al., 2014; Yang et al., 2011).

Moreover, studies knocking out essential autophagy genes in genetically engineered mouse models (GEMMs) for cancer have demonstrated a pro-tumorigenic role for autophagy (Guo et al., 2013b). Deletion of *Atg7* in $Kras^{G12D}$- and $Braf^{V600E}$-NSCLC in adult mice causes tumors to accumulate defective mitochondria and become metabolically impaired. Without ATG7, tumor cell proliferation is suppressed and tumors progress to benign oncocytomas rather than adenomas and carcinomas, extending the mice's lifespan (Guo et al., 2013a; Guo and White, 2013; Strohecker et al., 2013). In some but not all contexts autophagy promotes tumorigenesis by mitigating p53 activity (Guo et al., 2013a; Guo and White, 2013; Huo et al., 2013; Rao et al., 2014; Rosenfeldt et al., 2013; Strohecker et al., 2013; Yang et al., 2014).

Although these studies point to a pro-tumorigenic role for autophagy, they involved *Atg* gene deletion specifically in tumor cells, and thus do not demonstrate that autophagy deficiency is selectively detrimental to tumor tissue. Furthermore, as *Atg* gene deletion occurred concurrently with activation of oncogenic mutations that initiate tumorigenesis, these prior studies do not model

acute, systemic autophagy ablation as would occur during autophagy inhibition for cancer therapy.

To address the tumor selectivity of autophagy ablation in cancer, we engineered the mice to conditionally ([TAM])-inducible) and systemically delete *Atg7* throughout adult mice. We found that adult mice with *Atg7* acute whole-body deletion (*Atg7*$^{\Delta/\Delta}$ mice) manifested systemically blocked autophagy without extensive organ damage at 5 weeks post-deletion, although a small fraction of mice succumbed to *Streptococcus* infection. In contrast, by 6 to 12 weeks post deletion, extensive liver and muscle damage were evident and neurodegeneration limited survival to 2-3 months. *Atg7*$^{\Delta/\Delta}$ mice suffered lethality upon fasting, where mice displayed extreme muscle wasting and died of hypoglycemia, indicating that autophagy is required for glucose homeostasis. This reveals a new role for autophagy in the management of systemic energy balance. In the setting of cancer, 5 weeks of acute autophagy ablation converted established lung adenocarcinomas to oncocytomas and blocked mTOR and MAP kinase signaling, and cell proliferation and survival.

Compared to tumor-specific autophagy deficiency produced concurrently with tumor initiation, acute systemic autophagy ablation was more destructive to tumors. Thus, established tumors have greater autophagy dependency than both newly developing tumors and most normal tissues. To understand if the increased autophagy ablation sensitivity of these tumors only depends on the autophagy in the tumor, we evaluated the role of host autophagy in tumorigenesis. Host autophagy contributed to the growth of the tumors, probably

due to the role of autophagy providing nutrients that are essential for tumor progression. These findings suggest that, with proper control of the extent and/or timing of autophagy inhibition, there is likely to be a therapeutic window to suppress tumorigenesis while mostly sparing normal tissue.

Results

ATG7 deficiency does not alter lung tumor initiation

To test if autophagy influences tumor initiation, mice were engineered with Frt alleles of both *Kras*^{G12D} and *Trp53* (*p53*) without and with the conditional Floxed system for generating *Atg7*$^{\Delta/\Delta}$ mice. Mice can then have *Atg7* ablated by TAM administration and deletion of the Lox-P sites in the *Atg7* alleles by Cre recombinase followed later by initiation of lung tumorigenesis by intranasal administration of adenovirus expressing Flp recombinase (Ad-FLPo) and simultaneous activation of KRAS and deletion of *p53* by excision of Frt sites (Fig. 2.11A).

When *Atg7* was deleted and lung tumorigenesis was initiated by RAS activation and *p53* deletion, the number and size of tumors was monitored 4 and 8 weeks post-TAM (3 and 7 weeks post Ad-FLPo). There was no difference in tumor frequency or burden 3 weeks post Ad-FLPo regardless of *Atg7* status, indicating that the functional status of autophagy does not alter the ability of *Kras*^{G12D} activation and *p53* deficiency to induce formation of lung tumors (Fig. 2.11B-D). At 7 weeks post FLPo, however, there were fewer tumors and a reduction in tumor burden in *Atg7*$^{\Delta/\Delta}$ mice (Fig. 2.11D), coincident with emergence of oncocytomas rather than adenocarcinomas (Fig. 2.11B). This suggests that loss of autophagy does not affect the ability of activated RAS and *p53* deficiency to initiate tumorigenesis but rather it diminishes tumor growth over time.

Figure 2.11 Acute, systemic autophagy ablation does not alter the efficiency of tumor initiation.

A. Experimental design to induce conditional whole-body *Atg7* deletion prior to tumor induction. *Ubc-CreERT2*$^{/+}$*;Kras*$^{G12D\text{-}frt/+}$*;p53*$^{frt/frt}$*;Atg7*$^{+/+}$ and *Ubc-CreERT2*$^{/+}$*;Kras*$^{G12D\text{-}frt/+}$*;p53*$^{frt/frt}$*;Atg7*$^{flox/flox}$ mice were treated with TAM at 8-10 weeks of age by intraperitoneal injection to delete *Atg7* throughout the mouse, then these mice were infected with Ad-FLPo at 1 week post-TAM to activate RAS and delete *p53* and were analyzed at times thereafter.
B. Representative lung tumor histology (H&E) at 3 weeks post-Ad-FLPo, 4 weeks post-TAM (left) and 7 weeks post-Ad-FLPo, 8 weeks post-TAM (right). Arrows point to oncocytes.
C. Representative lung lobes at 7 weeks post-Ad-FLPo and 8 weeks post-TAM in the indicated genotypes.
D. Quantification of tumor numbers (left) and tumor burden (right) at the indicated times. Error bar represents SEM, *p≤0.05 (two-way ANOVA with Bonferroni post-test).

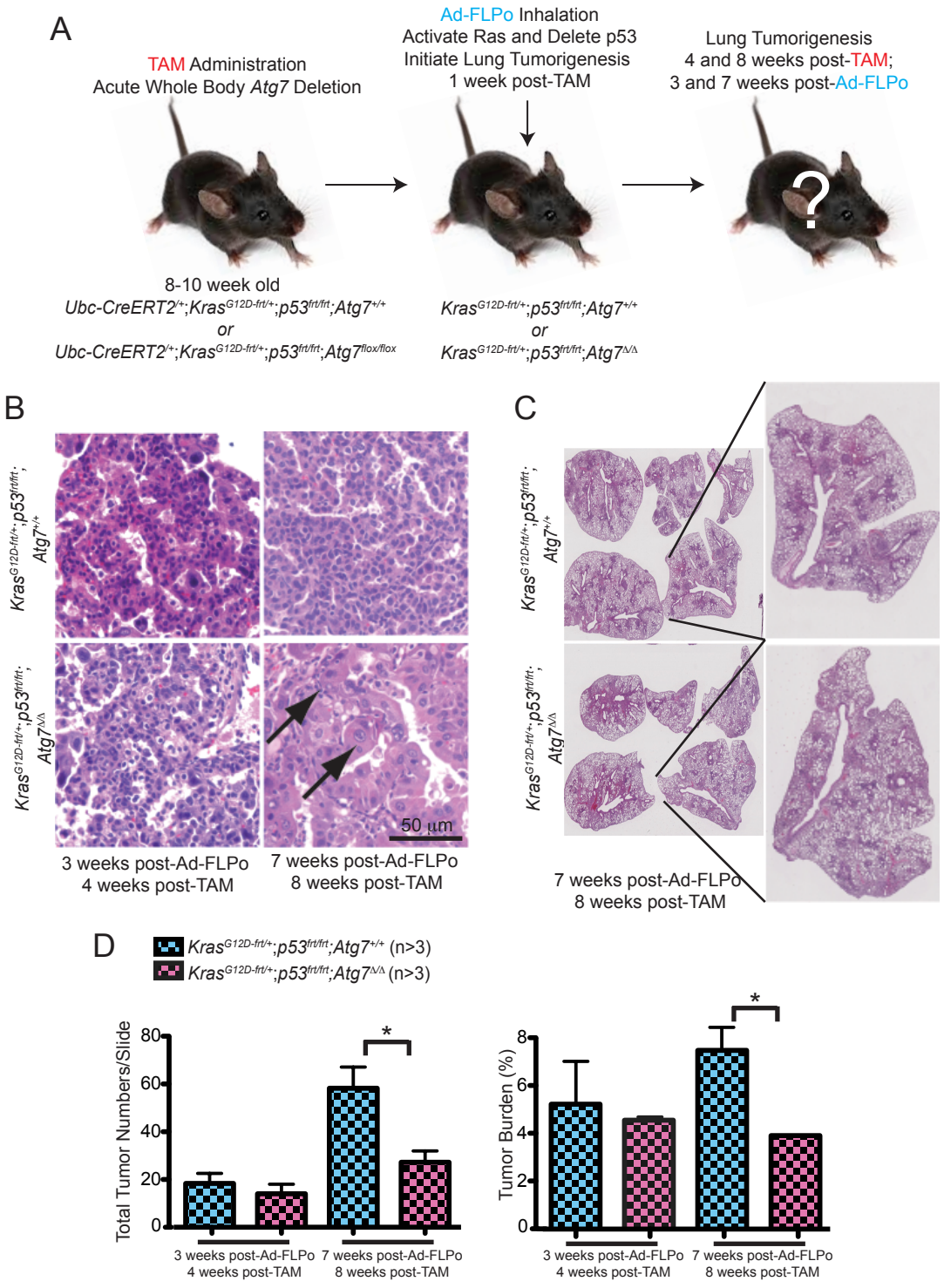

Figure 2.11 Acute, systemic autophagy ablation does not alter the efficiency of tumor initiation.

Acute ATG7 ablation alters tumor fate and compromises maintenance

To perform the converse experiment, lung tumors were generated, and at 12 weeks post-Ad-FLPo administration, TAM administration produced acute autophagy deficiency both in established tumors and normal tissues (Fig. 2.12A). Tumorigenesis was then assessed 5 weeks post-TAM (17 weeks post-Ad-FlpO) at which point there was little effect of autophagy ablation to normal tissues (Fig. 2.2A). Lung tumor burden was similar among all mice at the time of TAM administration as determined by micro-computed tomography (micro-CT) (Fig. 2.12B). At 17 weeks post-FLPo and 5 weeks post-TAM, as expected, lung tumor burden, with KRAS activation and *p53* deficiency produced large adenocarcinomas, encompassing most of the airspace in the lobes of the lungs with intact ATG7 (Fig. 2.12B-C). In contrast, in *Atg7*$^{\Delta/\Delta}$ mice at 17 weeks post FLPo and 5 weeks post-TAM, tumors were strikingly smaller, had poorly-defined margins, and were composed of oncocytes and dead tumor cells (Fig. 2.12B-C). There was no detectable difference in normal adjacent lung tissue in tumor-bearing *Atg7*$^{\Delta/\Delta}$ mice (Fig. 2.12B). The difference in tumor burden in *Atg7*$^{\Delta/\Delta}$ mice with 5 weeks of *Atg7* deletion was apparent by examination of wet lung weight and by determining tumor burden in scanned lung sections with tumor area reduced by one third (Fig. 2.12C-D).

Figure 2.12 Acute, systemic *Atg7* deficiency compromises tumorigenesis.

A. Experimental design to induce lung tumors prior to conditional whole-body *Atg7* deletion. *Ubc-CreERT2*$^{/+}$;*Kras*$^{G12D\text{-}frt/+}$;*p53*$^{frt/frt}$; *Atg7*$^{+/+}$ and *Ubc-CreERT2*$^{/+}$;*Kras*$^{G12D\text{-}frt/+}$;*p53*$^{frt/frt}$;*Atg7*$^{flox/flox}$ mice were infected with Ad-FLPo at 6-8 weeks of age to activate RAS and delete *p53*, then these mice were treated with TAM at 12 weeks post-Ad-FLPo by intraperitoneal injection to create *Atg7*$^{\Delta/\Delta}$ mice. Tumor progression was analyzed at various times thereafter.

B. Representative micro-CT 3-dimensional reconstruction and quantification of lung volume showing healthy air space before TAM treatment and equivalent tumor burden at the time of TAM treatment of mice with the indicated genotypes. *Kras*$^{+/+}$;*p53*$^{+/+}$;*Atg7*$^{+/+}$ mice were used as a control for normal lung airspace. Tumor histology and normal adjacent lung tissue (H&E images) were analyzed at 5 weeks post-TAM (last three panels). Arrows point to dead cells.

C. Representative low magnification tumor histology (H&E) at 17 weeks post-Ad-FLPo, 5 weeks post-TAM.

D. Quantification of wet lung weight (top) and tumor burden (bottom). Error bar represents SEM, p values are calculated using two-way ANOVA with Bonferroni post-test.

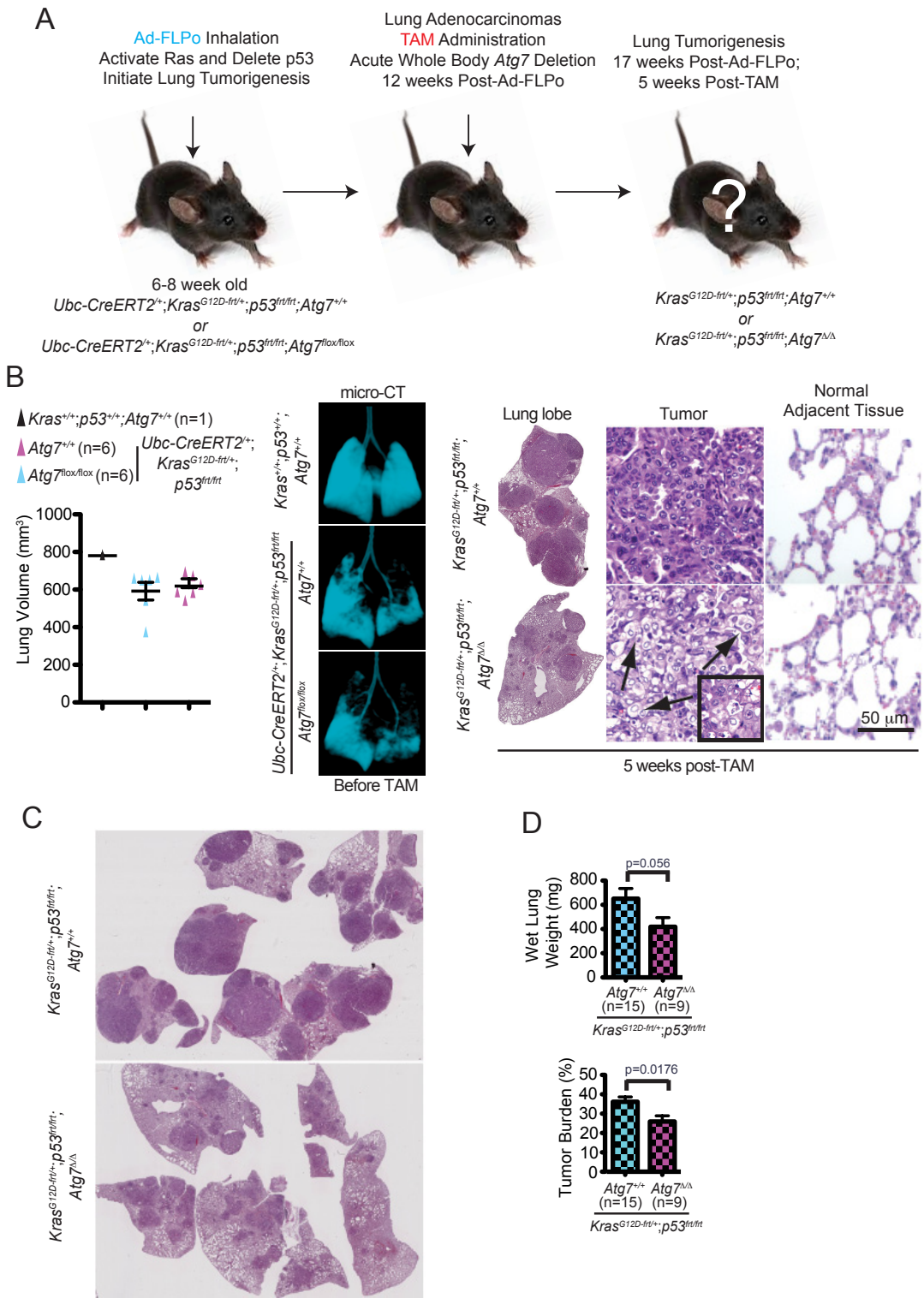

Figure 2.12 Acute, systemic *Atg7* deficiency compromises tumorigenesis.

Loss of ATG7 protein expression and autophagy ablation in tumors in the *Atg7*$^{\Delta/\Delta}$ mice were confirmed by Western blotting and immunohistochemistry (IHC). These tumors specifically accumulated p62 and LC3 aggregates, and abnormal mitochondria as detected by Tom20 IHC and electron microscopy (EM) (Fig. 2.13A-B). Tumors in *Atg7*$^{\Delta/\Delta}$ mice also displayed lipid accumulation (Fig. 2.13B) consistent with defective mitochondrial fatty acid oxidation as reported previously with tumor-specific *Atg7* deficiency (Guo et al., 2013a).

The impaired tumorigenesis in *Atg7*$^{\Delta/\Delta}$ mice was attributed to increased apoptosis (active CASPASE-3) (Fig. 2.13C) and ablation of proliferation, mTOR and MAP kinase signaling (KI67, loss of phosphorylated S6 [P-S6], 4E-BP1 [P-4E-BP1] and ERK [P-ERK] IHC) (Fig. 2.13 D-F). Serum glucose levels were similar in wild type and *Atg7*$^{\Delta/\Delta}$ tumor-bearing mice, indicating that hypoglycemia was not a factor contributing to defective tumor growth and survival (data not shown). While tumor-specific deletion of *Atg7* concurrently with tumor initiation by KRAS activation and *p53* deletion also reduces tumor burden, generates oncocytomas, suppresses proliferation and induces tumor cell death progressively beyond 6 weeks post deletion (Guo et al., 2013a), the kinetics and magnitude of these events are greatly accelerated by acute ablation of *Atg7* throughout the mouse (Fig. 2.14).

Figure 2.13 Acute autophagy ablation promotes apoptosis and compromises proliferation.

A. Representative western blotting for ATG7, p62, S6, P-S6 and LC3 of *Atg7*$^{+/+}$ or *Atg*$^{\Delta/\Delta}$ tumor tissues. β-ACTIN serves a protein loading control.
B. Representative IHC for ATG7, p62, TOM20, EM and Oil red O images of tumor tissue; and Oil red O of adjacent lung tissue. Arrows in second panel point to p62 aggregates and arrows in the third panel point to TOM20 accumulation in tumors from ATG7-deficient mice. N: nucleus, M: mitochondria, Ly: Lysosome, AP: Autophagosome, L: Lipid.
C. Representative IHC images for active CASPASE-3 (left) with quantification (right). Error bar represents SEM, p values are calculated using two-way ANOVA with Bonferroni post-test.
D. Representative IHC images for KI67 (left) with quantification (right). Error bar represents SEM, p values are calculated using two-way ANOVA with Bonferroni post-test.
E. Representative IHC images for S6, P-S6, 4E-BP1, P-4E-BP1, ERK and P-ERK.
F. Representative low magnification IHC images of P-S6, P-4E-BP1 and P-ERK IHC from Fig. 2.13E.

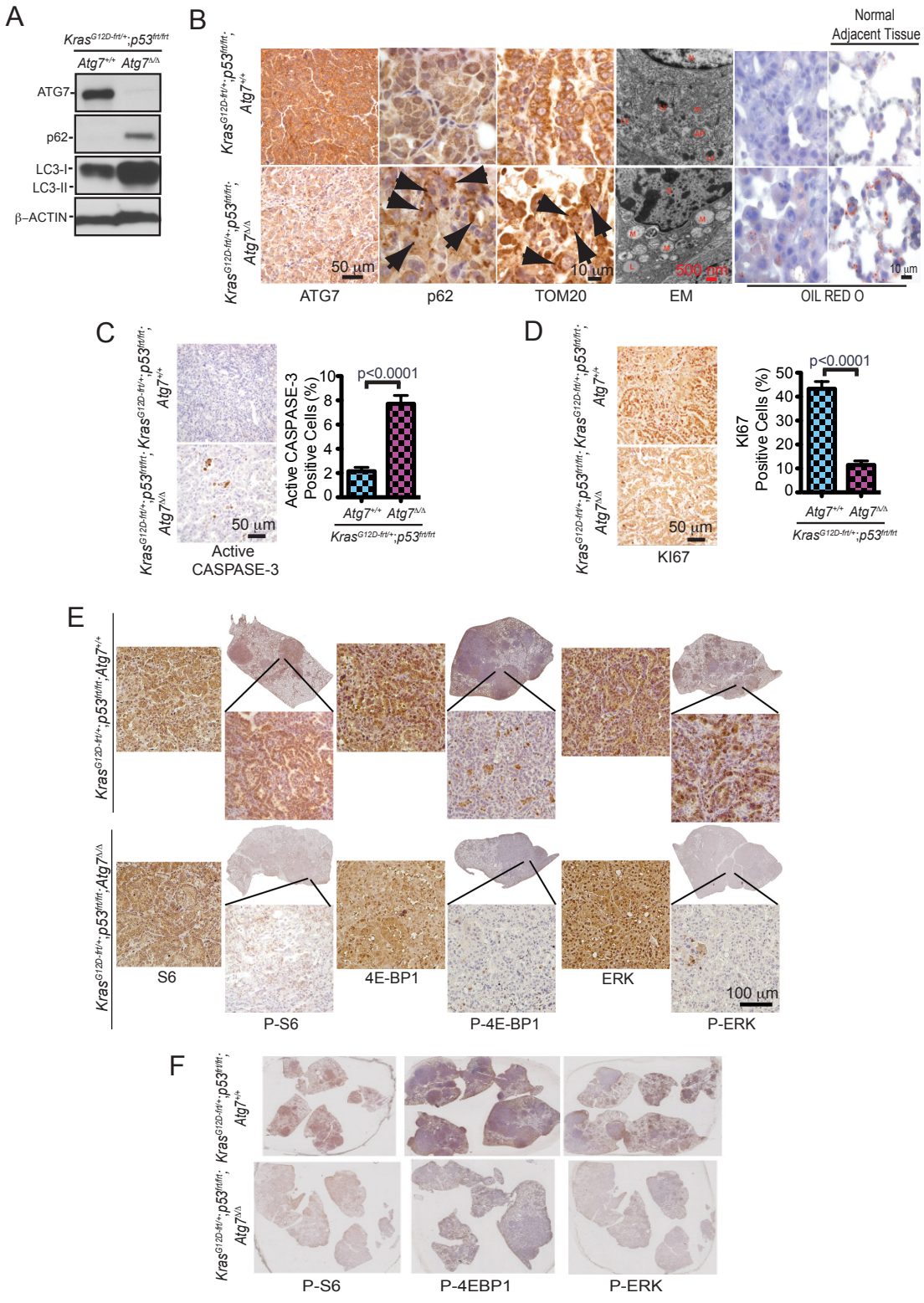

Figure 2.13 Acute autophagy ablation promotes apoptosis and compromises proliferation.

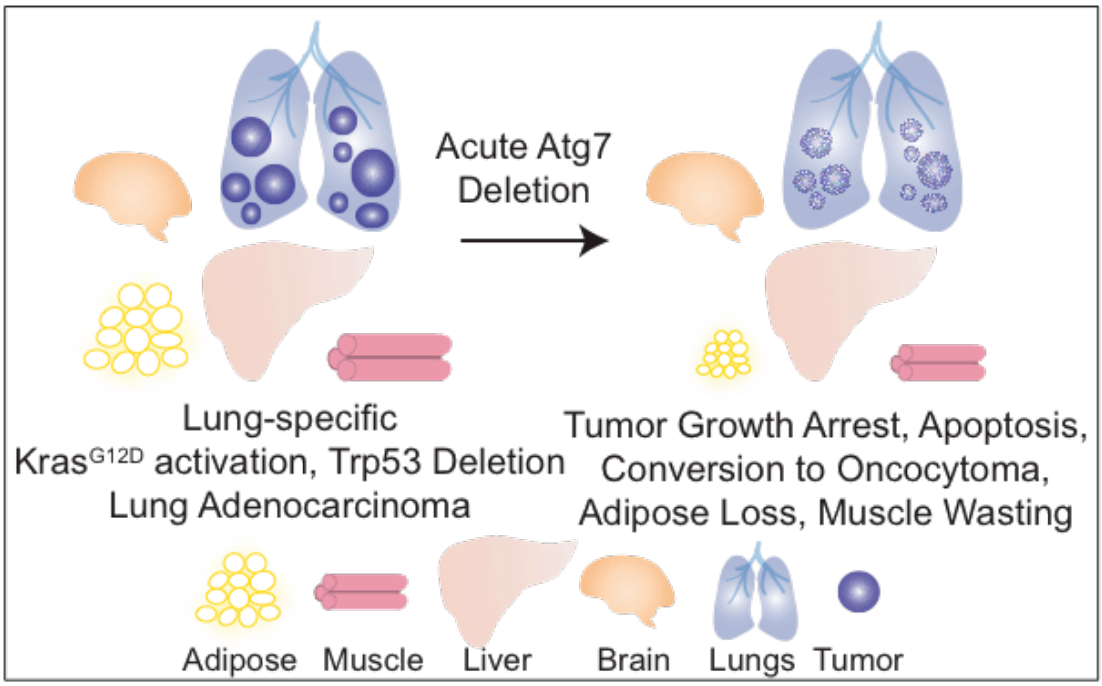

Figure 2.14 A model for destructive effect of autophagy on established tumors.

Host autophagy contributes tumorigenesis

To uncover the molecular basis of tumor-supporting role of autophagy, we investigated whether the autophagy in the host is important. By using the novel opportunity of the whole body autophagy conditional ablation model, we first switched off autophagy in the host, and then transplanted autophagy wild type TDCLs (Guo et al., 2013a) into autophagy-deficient or control wild type mice. We observed a dramatic difference in tumor growth; subcutaneous masses of tumors in autophagy-ablated host were smaller than tumors in autophagy intact host (Fig. 2.15A). Interestingly, tumor volume was not evenly occupied all with tumor cells in the autophagy deficient host and was instead tumor was composed

mainly stromal fibroblasts (Fig. 2.15B). This result indicates a novel role for host autophagy in promoting tumor growth.

Figure 2.15 Host autophagy contributes tumorigenesis.

A. Weights of the Atg7-wild type tumors in autophagy-intact (*Ubc-CreERT2/+*) or –deficient (*Atg7$^{\Delta/\Delta}$*) host at 3.5 weeks post-TDCL injection and 5 weeks post-TAM. Error bar represents SEM, *p≤0.05 (two-way ANOVA with Bonferroni post-test).

B. Representative histology (H&E) of the Atg7-wild type tumors in autophagy-intact (*Ubc-CreERT2/+*) or –deficient (*Atg7$^{\Delta/\Delta}$*) host at 3.5 weeks post-TDCL injection and 5 weeks post-TAM.

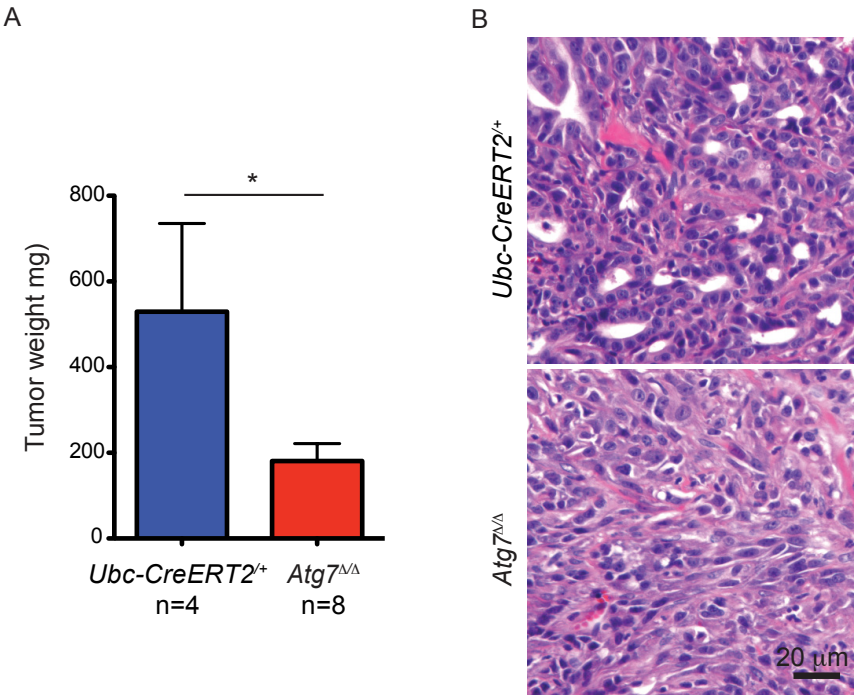

Figure 2.15 Host autophagy contributes tumorigenesis.

Discussion

RAS-driven cancers often upregulate autophagy and are dependent on autophagy for survival although the point at which autophagy functions during tumorigenesis was not known (Guo et al., 2013b). To address this, we ablated *Atg7* and then initiated tumorigenesis by activating RAS and deleting *p53* in the lung. Autophagy appeared dispensable for tumor initiation in this setting, although over time the suppressed proliferation and emergence of oncocytomas as seen previously in the lung tumor-specific *Atg7* knockouts were apparent (Karsli-Uzunbas et al., 2014). This suggests that functional autophagy status does not alter the efficiency by which $Kras^{G12D}$ activation and *p53* loss initiate lung tumor formation, but rather it is instead critical for tumor maintenance.

Acute knockdown of essential autophagy genes in many RAS mutant human cancer cell lines can rapidly suppress growth and survival, whereas knockout of essential autophagy genes in GEMMs at the time of cancer initiation suppresses tumor growth gradually over time (Guo et al., 2011; Guo et al., 2013a; Rao et al., 2014; Rosenfeldt et al., 2013; Yang et al., 2014; Yang et al., 2011). This indicates that acute autophagy ablation may be more detrimental to tumorigenesis than constitutive ablation. To test this hypothesis, *Atg7* was acutely ablated in mice with established $Kras^{G12D}$-activated and *p53*-deficient NSCLC. Five weeks of systemic autophagy deficiency was dramatically destructive to these pre-existing NSCLCs, which underwent loss of mTOR and MAP kinase signaling, proliferative arrest, apoptosis and conversion of adenocarcinomas to oncocytomas (Karsli-Uzunbas et al., 2014). Branched chain

amino acids and arginine are mTOR inducers and there were low levels of serum valine and arginine in response to autophagy inhibition, which may contribute to loss of mTOR signaling along with defective mitochondrial metabolism (Fig. 2.6A). Acute autophagy ablation more severely compromises tumorigenesis in comparison to tumors that evolve with deficiency in essential autophagy genes.

Established tumors may be more autophagy-dependent, systemic autophagy deficiency may be more destructive to tumors than tumor-specific deficiency, or tumors evolving without autophagy may have some capacity to adapt, diminishing the impact of autophagy loss. A possible explanation for destructive role of systemic autophagy inhibition might be defective host autophagy that is not able to replenish nutrients to feed cancer cells. In support of systemic autophagy deficiency being more detrimental to tumorigenesis, it also causes the elimination of WAT, perhaps creating a systemic environment metabolically unsupportive of tumor growth. In favor of these hypotheses, we should identify and target the nutrients, growth factors or any metabolites that are failed to circulate due to impaired autophagy.

CHAPTER 5

GENERAL DISCUSSION AND CONCLUSIONS

Autophagy and cancer have a complex relationship since the role of autophagy may differ in different tissues and different stages of disease. As a protection mechanism against genomic instability and tissue damage, autophagy may function as a tumor suppressor; but it can also sustain survival in metabolic stress by recycling components and ensuring homeostasis, thus it acts to promote tumor progression. RAS-driven cancer cells have increased levels of autophagy to sustain mitochondrial function for their metabolic needs. Autophagy deficiency in RAS-transformed cells causes accumulation of damaged mitochondria, generating metabolic problems incompatible with survival (Guo et al., 2011; Yang et al., 2011)

Additionally, if *Atg7* is deleted in KRAS- or BRAF-driven tumors, tumor progression is impaired and tumors display oncocytic changes instead of adenocarcinoma formation, by which proliferation is suppressed and tumor burden is reduced (Guo et al., 2013a; Strohecker et al., 2013). Oncocytomas are rare and benign tumor types characterized by accumulation of respiration defective mitochondria associated with mitochondrial genome mutations (Gasparre et al., 2011). If oncocytoma formation is induced due to autophagy inhibition, then autophagy defects may be an underlying basis for human oncocytomas and autophagy may be necessary to maintain adenocarcinoma fate. In favor of this idea, autophagy inhibition in lung cancer may limit tumor progression to benign disease. We have learned a lot from these previous studies, but one of the main limitations of these mouse models, as informative they are, autophagy ablation was only in tumor and only at the time of tumor

initiation. Furthermore, loss of autophagy can be destructive to some normal tissues, so whether or not autophagy inhibition would selectively compromise tumorigenesis while sparing normal tissue was unclear. For this reason, we generated a mouse model where we can induce tumor growth and systemically ablate autophagy independently.

To investigate the potential inhibitory role of autophagy ablation on tumorigenesis, we first examined the functional consequences of systemic whole body autophagy ablation in adult animals, by deleting Atg7 ubiquitously in all tissues. Acute autophagy inhibition was initially well tolerated with an exception of adipose tissue loss, but after 2-3 months, the animals ultimately succumbed to *Streptococcus* infection and neurodegeneration, and displayed damage to tissues such as liver, muscle and testis. *p53*, as a stress response gene, was induced in autophagy-deficient brains, likely as observed in autophagy ablated tumors (Guo et al., 2013a; Strohecker et al., 2013). Interestingly, deleting *p53* increased lifespan of Atg7-ablated mice, but did not restore the survival completely. Another remarkable observation was the effect of autophagy on p53-dependent tumor suppression; indicating ATG7 may inhibit p53 induction, and hence may contribute lymphoma growth. Since autophagy is required in stress survival in neonates, we wanted to identify if adult mice also require autophagy upon fasting. Indeed, autophagy deficient mice were intolerant to fasting and died of hypoglycemia. Completely different from that of neonates, mice were able to sustain serum amino acids likely by degrading muscle tissue. *p53* deletion did not rescue hypoglycemia that is caused by autophagy deficiency, but rescued

hypoglycemia-induced death. The mechanism by which ATG7 suppresses p53 is still an open question.

Our model clearly has potential to reflect the consequences of systemic autophagy inhibition. This raised an important question: is the tolerable short-term phase following autophagy ablation enough to selectively inhibit tumorigenesis? Efficiency of tumor initiation was the same if autophagy was inhibited prior to tumor induction, however growth impairment did occur later on. In contrast, the effect of systemic autophagy ablation was dramatic on established tumors; autophagy ablation impaired proliferation and increased apoptosis. Are established tumors more stressed or is microenvironmental autophagy more critical? This model gave us a novel opportunity to answer this question partially as to whether the host autophagy is important for tumor support. Indeed, host autophagy was essential tumor progression. Although the mechanism has yet to be determined, systemic autophagy probably provides nutrients, metabolites or growth factors required for tumor growth. If the targets, which need to be replenished by autophagy, are identified; then these might be new targets for cancer therapy. In addition to metabolic requirements, the role of autophagy in chromatin remodeling and differentiation should also be identified.

The key to determining if autophagy inhibition will be potentially effective to diminish tumorigenesis is to establish if tumors are more susceptible to acute autophagy inactivation than normal tissues, therefore providing a therapeutic window. Our data demonstrate that complete systemic autophagy inhibition for prolonged durations is not likely to be tolerable from a safety perspective. That

said, the most serious observed effects on normal health were bacterial infection and neurodegeneration. Infection can presumably be managed through prophylactic antibiotics, and central nervous system toxicities should be considered in the design of pharmacological agents. Note that, genetic ablation as we have done here is complete and irreversible inhibition of autophagy, not likely achievable with small molecule inhibitors and as such this represents an extreme situation. It would, however, be interesting to compare genetic and pharmacological inhibition of autophagy (with chloroquine, for example) to help establish how effective autophagy inhibition needs to be to impair tumor growth. To what extent the detrimental effects of acute autophagy ablation are reversible in normal and tumor tissue also remains to be addressed. Finally, it will be interesting to test systemic deletion of other autophagy-related genes in this model to resolve any potential autophagy-independent functions associated with loss of specific *Atg* genes. With these issues addressed, our observation that 5 weeks of acute *Atg7* ablation was sufficient to shut off mTOR and MAP kinase signaling and cause widespread tumor proliferative arrest and death while largely sparing normal tissues raises great hopes for antitumor efficacy.

REFERENCES

Aita, V.M., Liang, X.H., Murty, V.V., Pincus, D.L., Yu, W., Cayanis, E., Kalachikov, S., Gilliam, T.C., and Levine, B. (1999). Cloning and genomic organization of beclin 1, a candidate tumor suppressor gene on chromosome 17q21. Genomics *59*, 59-65.

Alvers, A.L., Wood, M.S., Hu, D., Kaywell, A.C., Dunn, W.A., Jr., and Aris, J.P. (2009). Autophagy is required for extension of yeast chronological life span by rapamycin. Autophagy *5*, 847-849.

Bjedov, I., Toivonen, J.M., Kerr, F., Slack, C., Jacobson, J., Foley, A., and Partridge, L. (2010). Mechanisms of life span extension by rapamycin in the fruit fly Drosophila melanogaster. Cell metabolism *11*, 35-46.

Boya, P., Gonzalez-Polo, R.A., Casares, N., Perfettini, J.L., Dessen, P., Larochette, N., Metivier, D., Meley, D., Souquere, S., Yoshimori, T.*, et al.* (2005). Inhibition of macroautophagy triggers apoptosis. Molecular and cellular biology *25*, 1025-1040.

Cemma, M., Kim, P.K., and Brumell, J.H. (2011). The ubiquitin-binding adaptor proteins p62/SQSTM1 and NDP52 are recruited independently to bacteria-associated microdomains to target Salmonella to the autophagy pathway. Autophagy *7*, 341-345.

Chan, E.Y. (2009). mTORC1 phosphorylates the ULK1-mAtg13-FIP200 autophagy regulatory complex. Science signaling *2*, pe51.

Cheong, H., Wu, J., Gonzales, L.K., Guttentag, S.H., Thompson, C.B., and Lindsten, T. (2014). Analysis of a lung defect in autophagy-deficient mouse strains. Autophagy *10*, 45-56.

Degenhardt, K., Mathew, R., Beaudoin, B., Bray, K., Anderson, D., Chen, G., Mukherjee, C., Shi, Y., Gelinas, C., Fan, Y.*, et al.* (2006). Autophagy promotes tumor cell survival and restricts necrosis, inflammation, and tumorigenesis. Cancer cell *10*, 51-64.

Dorn, B.R., Dunn, W.A., Jr., and Progulske-Fox, A. (2002). Bacterial interactions with the autophagic pathway. Cellular microbiology *4*, 1-10.

Ebato, C., Uchida, T., Arakawa, M., Komatsu, M., Ueno, T., Komiya, K., Azuma, K., Hirose, T., Tanaka, K., Kominami, E.*, et al.* (2008). Autophagy is important in islet homeostasis and compensatory increase of beta cell mass in response to high-fat diet. Cell metabolism *8*, 325-332.

Ezaki, J., Matsumoto, N., Takeda-Ezaki, M., Komatsu, M., Takahashi, K., Hiraoka, Y., Taka, H., Fujimura, T., Takehana, K., Yoshida, M.*, et al.* (2011).

Liver autophagy contributes to the maintenance of blood glucose and amino acid levels. Autophagy *7*, 727-736.

Feng, Z., Zhang, H., Levine, A.J., and Jin, S. (2005). The coordinate regulation of the p53 and mTOR pathways in cells. Proc Natl Acad Sci U S A *102*, 8204-8209.

Frankel, L.B., and Lund, A.H. (2012). MicroRNA regulation of autophagy. Carcinogenesis *33*, 2018-2025.

Fullgrabe, J., Klionsky, D.J., and Joseph, B. (2014). The return of the nucleus: transcriptional and epigenetic control of autophagy. Nature reviews Molecular cell biology *15*, 65-74.

Fung, C., Lock, R., Gao, S., Salas, E., and Debnath, J. (2008). Induction of autophagy during extracellular matrix detachment promotes cell survival. Molecular biology of the cell *19*, 797-806.

Gasparre, G., Romeo, G., Rugolo, M., and Porcelli, A.M. (2011). Learning from oncocytic tumors: Why choose inefficient mitochondria? Biochimica et biophysica acta *1807*, 633-642.

Geng, J., and Klionsky, D.J. (2008). The Atg8 and Atg12 ubiquitin-like conjugation systems in macroautophagy. 'Protein modifications: beyond the usual suspects' review series. EMBO reports *9*, 859-864.

Goldsmith, J., Levine, B., and Debnath, J. (2014). Autophagy and cancer metabolism. Methods in enzymology *542*, 25-57.

Guo, J.Y., Chen, H.Y., Mathew, R., Fan, J., Strohecker, A.M., Karsli-Uzunbas, G., Kamphorst, J.J., Chen, G., Lemons, J.M., Karantza, V.*, et al.* (2011). Activated Ras requires autophagy to maintain oxidative metabolism and tumorigenesis. Genes Dev *25*, 460-470.

Guo, J.Y., Karsli-Uzunbas, G., Mathew, R., Aisner, S.C., Kamphorst, J.J., Strohecker, A.M., Chen, G., Price, S., Lu, W., Teng, X.*, et al.* (2013a). Autophagy suppresses progression of K-ras-induced lung tumors to oncocytomas and maintains lipid homeostasis. Genes Dev *27*, 1447-1461.

Guo, J.Y., and White, E. (2013). Autophagy is required for mitochondrial function, lipid metabolism, growth and fate of KRAS (G12D) -driven lung tumors. Autophagy *9*.

Guo, J.Y., Xia, B., and White, E. (2013b). Autophagy-mediated tumor promotion. Cell *155*, 1216-1219.

Hamasaki, M., Shibutani, S.T., and Yoshimori, T. (2013). Up-to-date membrane biogenesis in the autophagosome formation. Current opinion in cell biology *25*, 455-460.

Hara, T., Nakamura, K., Matsui, M., Yamamoto, A., Nakahara, Y., Suzuki-Migishima, R., Yokoyama, M., Mishima, K., Saito, I., Okano, H.*, et al.* (2006). Suppression of basal autophagy in neural cells causes neurodegenerative disease in mice. Nature *441*, 885-889.

Harrison, D.E., Strong, R., Sharp, Z.D., Nelson, J.F., Astle, C.M., Flurkey, K., Nadon, N.L., Wilkinson, J.E., Frenkel, K., Carter, C.S.*, et al.* (2009). Rapamycin fed late in life extends lifespan in genetically heterogeneous mice. Nature *460*, 392-395.

He, C., and Levine, B. (2010). The Beclin 1 interactome. Current opinion in cell biology *22*, 140-149.

Huang, D.W., Sherman, B.T., and Lempicki, R.A. (2009). Systematic and integrative analysis of large gene lists using DAVID bioinformatics resources. Nat Protoc *4*, 44-57.

Huo, Y., Cai, H., Teplova, I., Bowman-Colin, C., Chen, G., Price, S., Barnard, N., Ganesan, S., Karantza, V., White, E.*, et al.* (2013). Autophagy opposes p53-mediated tumor barrier to facilitate tumorigenesis in a model of PALB2-associated hereditary breast cancer. Cancer discovery.

Jain, A., Lamark, T., Sjottem, E., Larsen, K.B., Awuh, J.A., Overvatn, A., McMahon, M., Hayes, J.D., and Johansen, T. (2010). p62/SQSTM1 is a target gene for transcription factor NRF2 and creates a positive feedback loop by inducing antioxidant response element-driven gene transcription. The Journal of biological chemistry *285*, 22576-22591.

Johansen, T., and Lamark, T. (2011). Selective autophagy mediated by autophagic adapter proteins. Autophagy *7*, 279-296.

Jung, C.H., Ro, S.H., Cao, J., Otto, N.M., and Kim, D.H. (2010). mTOR regulation of autophagy. FEBS letters *584*, 1287-1295.

Jung, H.S., Chung, K.W., Won Kim, J., Kim, J., Komatsu, M., Tanaka, K., Nguyen, Y.H., Kang, T.M., Yoon, K.H., Kim, J.W.*, et al.* (2008). Loss of autophagy diminishes pancreatic beta cell mass and function with resultant hyperglycemia. Cell metabolism *8*, 318-324.

Karantza-Wadsworth, V., Patel, S., Kravchuk, O., Chen, G., Mathew, R., Jin, S., and White, E. (2007). Autophagy mitigates metabolic stress and genome damage in mammary tumorigenesis. Genes Dev *21*, 1621-1635.

Karsli-Uzunbas, G., Guo, J.Y., Price, S., Teng, X., Laddha, S.V., Khor, S., Kalaany, N.Y., Jacks, T., Chan, C.S., Rabinowitz, J.D.*, et al.* (2014). Autophagy is required for glucose homeostasis and lung tumor maintenance. Cancer discovery *4*, 914-927.

Kim, J., Kim, Y.C., Fang, C., Russell, R.C., Kim, J.H., Fan, W., Liu, R., Zhong, Q., and Guan, K.L. (2013). Differential regulation of distinct Vps34 complexes by AMPK in nutrient stress and autophagy. Cell *152*, 290-303.

Kim, J., Kundu, M., Viollet, B., and Guan, K.L. (2011). AMPK and mTOR regulate autophagy through direct phosphorylation of Ulk1. Nature cell biology *13*, 132-141.

Kirkin, V., McEwan, D.G., Novak, I., and Dikic, I. (2009). A role for ubiquitin in selective autophagy. Molecular cell *34*, 259-269.

Komatsu, M., Kurokawa, H., Waguri, S., Taguchi, K., Kobayashi, A., Ichimura, Y., Sou, Y.S., Ueno, I., Sakamoto, A., Tong, K.I.*, et al.* (2010). The selective autophagy substrate p62 activates the stress responsive transcription factor Nrf2 through inactivation of Keap1. Nature cell biology *12*, 213-223.

Komatsu, M., Waguri, S., Chiba, T., Murata, S., Iwata, J., Tanida, I., Ueno, T., Koike, M., Uchiyama, Y., Kominami, E.*, et al.* (2006). Loss of autophagy in the central nervous system causes neurodegeneration in mice. Nature *441*, 880-884.

Komatsu, M., Waguri, S., Koike, M., Sou, Y.S., Ueno, T., Hara, T., Mizushima, N., Iwata, J., Ezaki, J., Murata, S.*, et al.* (2007). Homeostatic levels of p62 control cytoplasmic inclusion body formation in autophagy-deficient mice. Cell *131*, 1149-1163.

Komatsu, M., Waguri, S., Ueno, T., Iwata, J., Murata, S., Tanida, I., Ezaki, J., Mizushima, N., Ohsumi, Y., Uchiyama, Y.*, et al.* (2005). Impairment of starvation-induced and constitutive autophagy in Atg7-deficient mice. The Journal of cell biology *169*, 425-434.

Kuma, A., Hatano, M., Matsui, M., Yamamoto, A., Nakaya, H., Yoshimori, T., Ohsumi, Y., Tokuhisa, T., and Mizushima, N. (2004). The role of autophagy during the early neonatal starvation period. Nature *432*, 1032-1036.

Laddha, S.V., Ganesan, S., Chan, C.S., and White, E. (2014). Mutational landscape of the essential autophagy gene BECN1 in human cancers. Molecular cancer research : MCR *12*, 485-490.

Lee, I.H., Cao, L., Mostoslavsky, R., Lombard, D.B., Liu, J., Bruns, N.E., Tsokos, M., Alt, F.W., and Finkel, T. (2008). A role for the NAD-dependent deacetylase Sirt1 in the regulation of autophagy. Proc Natl Acad Sci U S A *105*, 3374-3379.

Levine, B., and Kroemer, G. (2008). Autophagy in the pathogenesis of disease. Cell *132*, 27-42.

Levy, J.M., Thompson, J.C., Griesinger, A.M., Amani, V., Donson, A.M., Birks, D.K., Morgan, M.J., Mirsky, D.M., Handler, M.H., Foreman, N.K.*, et al.* (2014). Autophagy inhibition improves chemosensitivity in BRAF(V600E) brain tumors. Cancer discovery *4*, 773-780.

Liang, X.H., Kleeman, L.K., Jiang, H.H., Gordon, G., Goldman, J.E., Berry, G., Herman, B., and Levine, B. (1998). Protection against fatal Sindbis virus encephalitis by beclin, a novel Bcl-2-interacting protein. Journal of virology *72*, 8586-8596.

Lindqvist, L.M., and Vaux, D.L. (2014). BCL2 and related prosurvival proteins require BAK1 and BAX to affect autophagy. Autophagy *10*, 1474-1475.

Lippai, M., and Low, P. (2014). The role of the selective adaptor p62 and ubiquitin-like proteins in autophagy. BioMed research international *2014*, 832704.

Liu, K., and Czaja, M.J. (2013). Regulation of lipid stores and metabolism by lipophagy. Cell death and differentiation *20*, 3-11.

Lock, R., Kenific, C.M., Leidal, A.M., Salas, E., and Debnath, J. (2014). Autophagy dependent production of secreted factors facilitates oncogenic RAS-driven invasion. Cancer discovery.

Mancias, J.D., Wang, X., Gygi, S.P., Harper, J.W., and Kimmelman, A.C. (2014). Quantitative proteomics identifies NCOA4 as the cargo receptor mediating ferritinophagy. Nature *509*, 105-109.

Manjithaya, R., Nazarko, T.Y., Farre, J.C., and Subramani, S. (2010). Molecular mechanism and physiological role of pexophagy. FEBS letters *584*, 1367-1373.

Martinez-Outschoorn, U.E., Trimmer, C., Lin, Z., Whitaker-Menezes, D., Chiavarina, B., Zhou, J., Wang, C., Pavlides, S., Martinez-Cantarin, M.P., Capozza, F.*, et al.* (2010). Autophagy in cancer associated fibroblasts promotes tumor cell survival: Role of hypoxia, HIF1 induction and NFkappaB activation in the tumor stromal microenvironment. Cell cycle *9*, 3515-3533.

Masiero, E., Agatea, L., Mammucari, C., Blaauw, B., Loro, E., Komatsu, M., Metzger, D., Reggiani, C., Schiaffino, S., and Sandri, M. (2009). Autophagy is required to maintain muscle mass. Cell metabolism *10*, 507-515.

Mathew, R., Khor, S., Hackett, S.R., Rabinowitz, J.D., Perlman, D.H., and White, E. (2014). Functional role of autophagy-mediated proteome remodeling in cell survival signaling and innate immunity. Molecular cell *55*, 916-930.

Mathew, R., Kongara, S., Beaudoin, B., Karp, C.M., Bray, K., Degenhardt, K., Chen, G., Jin, S., and White, E. (2007). Autophagy suppresses tumor progression by limiting chromosomal instability. Genes Dev *21*, 1367-1381.

Meijer, A.J., and Klionsky, D.J. (2011). Vps34 is a phosphatidylinositol 3-kinase, not a phosphoinositide 3-kinase. Autophagy *7*, 563-564.

Mizushima, N., and Komatsu, M. (2011). Autophagy: renovation of cells and tissues. Cell *147*, 728-741.

Mizushima, N., and Levine, B. (2010). Autophagy in mammalian development and differentiation. Nature cell biology *12*, 823-830.

Mizushima, N., Yamamoto, A., Matsui, M., Yoshimori, T., and Ohsumi, Y. (2004). In vivo analysis of autophagy in response to nutrient starvation using transgenic mice expressing a fluorescent autophagosome marker. Molecular biology of the cell *15*, 1101-1111.

Mortensen, M., Ferguson, D.J., Edelmann, M., Kessler, B., Morten, K.J., Komatsu, M., and Simon, A.K. (2010). Loss of autophagy in erythroid cells leads to defective removal of mitochondria and severe anemia in vivo. Proc Natl Acad Sci U S A *107*, 832-837.

Mortimore, G.E., and Poso, A.R. (1987). Intracellular protein catabolism and its control during nutrient deprivation and supply. Annual review of nutrition *7*, 539-564.

Nakagawa, I., Amano, A., Mizushima, N., Yamamoto, A., Yamaguchi, H., Kamimoto, T., Nara, A., Funao, J., Nakata, M., Tsuda, K.*, et al.* (2004). Autophagy defends cells against invading group A Streptococcus. Science *306*, 1037-1040.

Neff, F., Flores-Dominguez, D., Ryan, D.P., Horsch, M., Schroder, S., Adler, T., Afonso, L.C., Aguilar-Pimentel, J.A., Becker, L., Garrett, L.*, et al.* (2013). Rapamycin extends murine lifespan but has limited effects on aging. J Clin Invest *123*, 3272-3291.

Ni, H.M., Boggess, N., McGill, M.R., Lebofsky, M., Borude, P., Apte, U., Jaeschke, H., and Ding, W.X. (2012). Liver-specific loss of Atg5 causes persistent activation of Nrf2 and protects against acetaminophen-induced liver injury. Toxicological sciences : an official journal of the Society of Toxicology *127*, 438-450.

Niture, S.K., and Jaiswal, A.K. (2012). Nrf2 protein up-regulates antiapoptotic protein Bcl-2 and prevents cellular apoptosis. The Journal of biological chemistry *287*, 9873-9886.

Nixon, R.A. (2013). The role of autophagy in neurodegenerative disease. Nature medicine *19*, 983-997.

Novak, I., Kirkin, V., McEwan, D.G., Zhang, J., Wild, P., Rozenknop, A., Rogov, V., Lohr, F., Popovic, D., Occhipinti, A.*, et al.* (2010). Nix is a selective autophagy receptor for mitochondrial clearance. EMBO reports *11*, 45-51.

Peng, Y.F., Shi, Y.H., Ding, Z.B., Ke, A.W., Gu, C.Y., Hui, B., Zhou, J., Qiu, S.J., Dai, Z., and Fan, J. (2013). Autophagy inhibition suppresses pulmonary metastasis of HCC in mice via impairing anoikis resistance and colonization of HCC cells. Autophagy *9*, 2056-2068.

Qu, X., Yu, J., Bhagat, G., Furuya, N., Hibshoosh, H., Troxel, A., Rosen, J., Eskelinen, E.L., Mizushima, N., Ohsumi, Y.*, et al.* (2003). Promotion of tumorigenesis by heterozygous disruption of the beclin 1 autophagy gene. J Clin Invest *112*, 1809-1820.

Rabinowitz, J.D., and White, E. (2010). Autophagy and metabolism. Science *330*, 1344-1348.

Rao, S., Tortola, L., Perlot, T., Wirnsberger, G., Novatchkova, M., Nitsch, R., Sykacek, P., Frank, L., Schramek, D., Komnenovic, V.*, et al.* (2014). A dual role for autophagy in a murine model of lung cancer. Nature communications *5*, 3056.

Rea, S.L., Majcher, V., Searle, M.S., and Layfield, R. (2014). SQSTM1 mutations--bridging Paget disease of bone and ALS/FTLD. Experimental cell research *325*, 27-37.

Reggiori, F., and Klionsky, D.J. (2013). Autophagic processes in yeast: mechanism, machinery and regulation. Genetics *194*, 341-361.

Rosenfeldt, M.T., O'Prey, J., Morton, J.P., Nixon, C., MacKay, G., Mrowinska, A., Au, A., Rai, T.S., Zheng, L., Ridgway, R.*, et al.* (2013). p53 status determines the role of autophagy in pancreatic tumour development. Nature *504*, 296-300.

Rubinsztein, D.C., Codogno, P., and Levine, B. (2012). Autophagy modulation as a potential therapeutic target for diverse diseases. Nature reviews Drug discovery *11*, 709-730.

Rubinsztein, D.C., Marino, G., and Kroemer, G. (2011). Autophagy and aging. Cell *146*, 682-695.

Ruzankina, Y., Pinzon-Guzman, C., Asare, A., Ong, T., Pontano, L., Cotsarelis, G., Zediak, V.P., Velez, M., Bhandoola, A., and Brown, E.J. (2007). Deletion of the developmentally essential gene ATR in adult mice leads to age-related phenotypes and stem cell loss. Cell stem cell *1*, 113-126.

Saitsu, H., Nishimura, T., Muramatsu, K., Kodera, H., Kumada, S., Sugai, K., Kasai-Yoshida, E., Sawaura, N., Nishida, H., Hoshino, A.*, et al.* (2013). De novo mutations in the autophagy gene WDR45 cause static encephalopathy of childhood with neurodegeneration in adulthood. Nature genetics *45*, 445-449, 449e441.

Salem, A.F., Whitaker-Menezes, D., Lin, Z., Martinez-Outschoorn, U.E., Tanowitz, H.B., Al-Zoubi, M.S., Howell, A., Pestell, R.G., Sotgia, F., and Lisanti, M.P. (2012). Two-compartment tumor metabolism: autophagy in the tumor microenvironment and oxidative mitochondrial metabolism (OXPHOS) in cancer cells. Cell cycle *11*, 2545-2556.

Sancak, Y., Bar-Peled, L., Zoncu, R., Markhard, A.L., Nada, S., and Sabatini, D.M. (2010). Ragulator-Rag complex targets mTORC1 to the lysosomal surface and is necessary for its activation by amino acids. Cell *141*, 290-303.

Satoo, K., Noda, N.N., Kumeta, H., Fujioka, Y., Mizushima, N., Ohsumi, Y., and Inagaki, F. (2009). The structure of Atg4B-LC3 complex reveals the mechanism of LC3 processing and delipidation during autophagy. The EMBO journal *28*, 1341-1350.

Scherz-Shouval, R., Shvets, E., Fass, E., Shorer, H., Gil, L., and Elazar, Z. (2007). Reactive oxygen species are essential for autophagy and specifically regulate the activity of Atg4. The EMBO journal *26*, 1749-1760.

Schiaffino, S., Dyar, K.A., Ciciliot, S., Blaauw, B., and Sandri, M. (2013). Mechanisms regulating skeletal muscle growth and atrophy. The FEBS journal *280*, 4294-4314.

Schneider, J.L., and Cuervo, A.M. (2014). Autophagy and human disease: emerging themes. Current opinion in genetics & development *26C*, 16-23.

Settembre, C., Di Malta, C., Polito, V.A., Garcia Arencibia, M., Vetrini, F., Erdin, S., Erdin, S.U., Huynh, T., Medina, D., Colella, P.*, et al.* (2011). TFEB links autophagy to lysosomal biogenesis. Science *332*, 1429-1433.

Singh, M., Lima, A., Molina, R., Hamilton, P., Clermont, A.C., Devasthali, V., Thompson, J.D., Cheng, J.H., Bou Reslan, H., Ho, C.C.*, et al.* (2010). Assessing therapeutic responses in Kras mutant cancers using genetically engineered mouse models. Nature biotechnology *28*, 585-593.

Singh, R., and Cuervo, A.M. (2012). Lipophagy: connecting autophagy and lipid metabolism. International journal of cell biology *2012*, 282041.

Singh, R., Kaushik, S., Wang, Y., Xiang, Y., Novak, I., Komatsu, M., Tanaka, K., Cuervo, A.M., and Czaja, M.J. (2009a). Autophagy regulates lipid metabolism. Nature *458*, 1131-1135.

Singh, R., Xiang, Y., Wang, Y., Baikati, K., Cuervo, A.M., Luu, Y.K., Tang, Y., Pessin, J.E., Schwartz, G.J., and Czaja, M.J. (2009b). Autophagy regulates adipose mass and differentiation in mice. J Clin Invest *119*, 3329-3339.

Strohecker, A.M., Guo, J.Y., Karsli-Uzunbas, G., Price, S.M., Chen, G.J., Mathew, R., McMahon, M., and White, E. (2013). Autophagy sustains mitochondrial glutamine metabolism and growth of BrafV600E-driven lung tumors. Cancer discovery *3*, 1272-1285.

Takamura, A., Komatsu, M., Hara, T., Sakamoto, A., Kishi, C., Waguri, S., Eishi, Y., Hino, O., Tanaka, K., and Mizushima, N. (2011). Autophagy-deficient mice develop multiple liver tumors. Genes Dev *25*, 795-800.

Tasdemir, E., Maiuri, M.C., Galluzzi, L., Vitale, I., Djavaheri-Mergny, M., D'Amelio, M., Criollo, A., Morselli, E., Zhu, C., Harper, F.*, et al.* (2008). Regulation of autophagy by cytoplasmic p53. Nature cell biology *10*, 676-687.

Terman, A., and Brunk, U.T. (2005). Autophagy in cardiac myocyte homeostasis, aging, and pathology. Cardiovascular research *68*, 355-365.

Tsukada, M., and Ohsumi, Y. (1993). Isolation and characterization of autophagy-defective mutants of Saccharomyces cerevisiae. FEBS letters *333*, 169-174.

Tsukamoto, S., Kuma, A., Murakami, M., Kishi, C., Yamamoto, A., and Mizushima, N. (2008). Autophagy is essential for preimplantation development of mouse embryos. Science *321*, 117-120.

Watson, R.O., Manzanillo, P.S., and Cox, J.S. (2012). Extracellular M. tuberculosis DNA targets bacteria for autophagy by activating the host DNA-sensing pathway. Cell *150*, 803-815.

Webb, A.E., and Brunet, A. (2014). FOXO transcription factors: key regulators of cellular quality control. Trends in biochemical sciences *39*, 159-169.

Webb, J.L., Ravikumar, B., Atkins, J., Skepper, J.N., and Rubinsztein, D.C. (2003). Alpha-Synuclein is degraded by both autophagy and the proteasome. The Journal of biological chemistry *278*, 25009-25013.

Wei, H., Wei, S., Gan, B., Peng, X., Zou, W., and Guan, J.L. (2011). Suppression of autophagy by FIP200 deletion inhibits mammary tumorigenesis. Genes Dev *25*, 1510-1527.

White, E. (2012). Deconvoluting the context-dependent role for autophagy in cancer. Nature reviews Cancer *12*, 401-410.

Wruck, C.J., Streetz, K., Pavic, G., Gotz, M.E., Tohidnezhad, M., Brandenburg, L.O., Varoga, D., Eickelberg, O., Herdegen, T., Trautwein, C.*, et al.* (2011). Nrf2 induces interleukin-6 (IL-6) expression via an antioxidant response element within the IL-6 promoter. The Journal of biological chemistry *286*, 4493-4499.

Yang, A., Rajeshkumar, N.V., Wang, X., Yabuuchi, S., Alexander, B.M., Chu, G.C., Von Hoff, D.D., Maitra, A., and Kimmelman, A.C. (2014). Autophagy is critical for pancreatic tumor growth and progression in tumors with p53 alterations. Cancer discovery *4*, 905-913.

Yang, L., Li, P., Fu, S., Calay, E.S., and Hotamisligil, G.S. (2010). Defective hepatic autophagy in obesity promotes ER stress and causes insulin resistance. Cell metabolism *11*, 467-478.

Yang, S., Wang, X., Contino, G., Liesa, M., Sahin, E., Ying, H., Bause, A., Li, Y., Stommel, J.M., Dell'antonio, G.*, et al.* (2011). Pancreatic cancers require autophagy for tumor growth. Genes Dev *25*, 717-729.

Yang, Z., and Klionsky, D.J. (2010). Mammalian autophagy: core molecular machinery and signaling regulation. Current opinion in cell biology *22*, 124-131.

Yi, C., Ma, M., Ran, L., Zheng, J., Tong, J., Zhu, J., Ma, C., Sun, Y., Zhang, S., Feng, W.*, et al.* (2012). Function and molecular mechanism of acetylation in autophagy regulation. Science *336*, 474-477.

Young, N.P., Crowley, D., and Jacks, T. (2011). Uncoupling cancer mutations reveals critical timing of p53 loss in sarcomagenesis. Cancer research *71*, 4040-4047.

Zhang, Y., Goldman, S., Baerga, R., Zhao, Y., Komatsu, M., and Jin, S. (2009). Adipose-specific deletion of autophagy-related gene 7 (atg7) in mice reveals a role in adipogenesis. Proc Natl Acad Sci U S A *106*, 19860-19865.

Zheng, Y.T., Shahnazari, S., Brech, A., Lamark, T., Johansen, T., and Brumell, J.H. (2009). The adaptor protein p62/SQSTM1 targets invading bacteria to the autophagy pathway. Journal of immunology *183*, 5909-5916.